

Laborde et al. Soft Sediment Deformations in the UK

1 **Do soft sediment deformations in the Late Triassic and Early Jurassic of the UK record seismic** 2 **activity during the break-up of Pangea?**

3
4 Marine Laborde-Casadaban^a, Catherine Homberg^a, Johann Schnyder^{a*}, Sandra Borderie^b and
5 Robert Raine^c

6 *^aLaboratoire IStEP, UMR 7193, case courrier 129, Sorbonne Université, CNRS, 4, pl. Jussieu, 75000,*
7 *Paris, France.*

8 *^bUnit of Earth Sciences, Geosciences Department, University of Fribourg, Chemin du Musée 6, 1700*
9 *Fribourg, Switzerland.*

10 *^cGeological Survey of Northern Ireland, Dundonald House, Upper Newtownards Road, BT4 3SB,*
11 *Belfast, Northern Ireland*

12
13 *Corresponding author: johann.schnyder@sorbonne-universite.fr

14
15 Key Words: Soft sediment deformations, seismites, Rhaetian, Hettangian, Triassic-Jurassic boundary

16 17 **Abstract**

18 The lagoonal and shallow marine sediments of the Penarth Group in the UK span the Triassic–Jurassic
19 boundary. These sediments contain several disturbed levels with soft sediment deformations (SSDs),
20 such as synsedimentary faults, injective domes, recumbent folds and slumps that are recognised in
21 most basins from SW England and South Wales to NW Northern Ireland. Field observations, notably
22 the closed link of the SSDs to active faults, attest an earthquake origin of the SSDs. Fluids, faults,
23 overpressure and lithology guided the style of the SSDs and their distribution in the sedimentary pile.
24 Analysis of the directional data relating to SSDs in each disturbed level shows preferred orientations
25 of deformation, which correspond to the local state of stress at the time. We favour a series of
26 earthquakes, rather than a single mega-event as a trigger of the observed features. The active local
27 extensional tectonic context was driven by the opening of the Permo-Triassic basins in Western
28 Europe. The data from the SSDs in the UK suggest the development of a multi-directional, mosaic-
29 style extensional context to occur during this early phase of the break-up of Pangea. Our integrated
30 tectonic/sedimentary study suggests that directional data from faults, injective domes, recumbent
31 folds and slumps preserved in sediments are reliable to reconstruct past seismic activity and basin
32 geodynamics.

33 34 **1. Introduction**

35 Soft sediment deformations (SSDs) are observed in almost all types of environments, from alluvial
36 fan and fluvial systems (Plaziat, 1998); shallow marine and tidal (Pope et al., 1997; Schnyder et al.,

37 2005; Greb and Archer, 2007; Ghosh et al., 2012); lacustrine (Marco et al., 1996; Ken-Tor et al., 2001)
38 and deep marine – turbidite environments (Allen, 1977; Bergerat et al., 2011; Homberg et al., 2013;
39 Basilone et al., 2015). These deformations include convolute bedding, overturned cross-stratification,
40 load structures or water escape features. Due to their low cohesion and small grain size with large
41 water content, silts are particularly sensitive to liquefaction (Allen 1977). During liquefaction, the
42 pore-fluid pressure increases and the grain weights are transferred to the fluid. This causes the loss
43 of grain packing and thus of the internal sediment organisation (Lowe, 1975, 1976; Allen, 1977). The
44 association of liquefaction with a driving force, such as gravity, an unstable density gradient or a
45 shear stress leads to the deformation of the original sedimentary deposit (Owen, 1987). Numerous
46 triggers may cause the liquefaction of sediments such as: (1) tsunamis (Takashimizu and Masuda,
47 2000; Nanayama et al., 2000; Schnyder et al., 2005; Le Roux et al., 2008), (2) tidal flux and tidal bores
48 (Tessier and Terwindt, 1994; Greb and Archer, 2007), (3) storm waves and breaking waves (Molina et
49 al. , 1998) or (4) rapid sedimentation and loading (Allen, 1982). **Earthquake(s) as a trigger of the**
50 **observed SSDs is frequently proposed in the literature**, yet in many cases the liquefaction is
51 attributed to a seismic shock without sufficient evidence (Pope et al., 1997; Kullberg et al., 2001).
52 This shows the difficulty in identifying earthquakes as the cause of sediment liquefaction without
53 well-defined and self-sufficient criteria. Several authors have shown that assigning earthquakes as
54 causing SSDs requires a number of criteria (Wheeler, 2002; Owen and Moretti, 2011), including:

55

- 56 (1) The occurrence of liquefied sediment layers,
- 57 (2) A large extent of synchronous liquefied event,
- 58 (3) A lateral continuity of a deformed bed along the outcrop,
- 59 (4) Similar structures to those observed during recent earthquakes (Audemard and De Santis, 1991;
60 Dechen and Aiping, 2012),
- 61 (5) The superposition of SSD levels in the sedimentary pile which may correspond to a succession of
62 seismic events. This criterion is especially strong when it is possible to link the deformed levels to
63 historical earthquakes (Marco et al., 1996; Ken-Tor et al., 2001),
- 64 (6) A sedimentary and tectonic context consistent with the occurrence of frequent earthquakes
65 (Bergerat et al., 2011).

66 Nevertheless, none of these criteria are direct evidence of earthquakes as a trigger. Indeed, very few
67 studies show the direct relationship between syn-sedimentary faults and SSDs (Basilone et al., 2015).

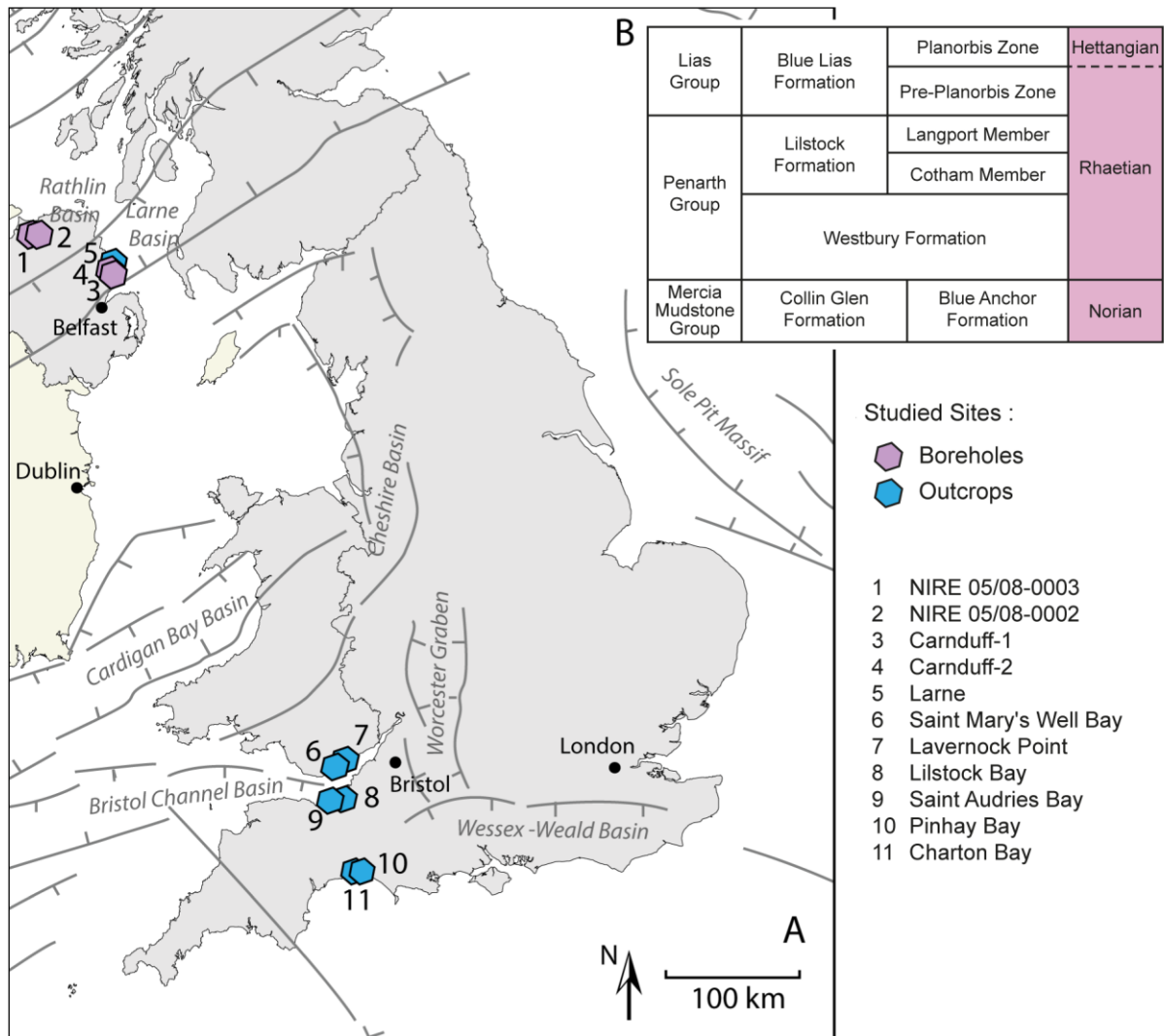
68 The Triassic-Jurassic boundary strata from the UK are affected by numerous soft deformation
69 structures recorded at a large scale (Richardson, 1911; Hallam, 1960; Mayall, 1983; Gallois, 2005,
70 2007, 2009). Several authors (Mayall, 1983; Hesselbo et al., 2002, 2004; Simms, 2003, 2007) assigned

71 those SSDs to earthquakes but the number of events and their origin are still debated. This study
72 investigates how the orientation of various SSDs are likely to inform on the SSDs trigger in Triassic–
73 Jurassic boundary strata from Southern England, South Wales and Northern Ireland. In the following,
74 we combined sedimentological and structural approaches to investigate the geometry, cross-cutting
75 relationships and distribution of the observed SSDs (faults, folds, slumps, domes), in order to assess
76 the possible earthquake trigger of the disturbed layers and to discuss the relationships of these
77 deformations with the Triassic–Jurassic rifting context.

78

79 **2. Geological context at the Triassic-Jurassic boundary in the UK**

80 The break-up of the supercontinent Pangea resulted in the opening of the Neotethys Ocean to the
81 east during the Late Permian – Early Triassic times (Ziegler and Stampfli, 2001). In north-western
82 Europe, numerous sedimentary basins related to this large-scale extensional tectonic context, and
83 often bounded by reactivated Palaeozoic faults, formed during the Triassic-Early Jurassic (Ziegler and
84 Dezes, 2006). This is the case for the N–S Worcester Basin, the E–W oriented Bristol Channel and
85 Wessex basins and the ENE-WSW oriented Lough Foyle and Larne basins (Figure 1A, Chadwick, 1993;
86 Holdsworth et al., 2012). Subsidence of these intracratonic basins continued during Jurassic and
87 Cretaceous times.



88
89 Figure 1. Tectonic framework of the UK at the Triassic–Jurassic transition. A: Location of studied sites.

90 The faults which mark the different Permo-Triassic basins are those defined by Holdsworth et al.
91 (2012). B: Lithostratigraphy of the Triassic-Jurassic boundary deposits in the UK. After Warrington et
92 al. (1994) and Mitchell (2004).

93 The sediments preserved in the UK basins recorded a long-term transgressive period extending from
94 the Late Triassic until the Early Jurassic (Warrington et al., 1980), starting with the continental
95 floodplain and lake deposits of the Mercia Mudstone Group of Triassic age. In England, the upper
96 unit of the Mercia Mudstone Group corresponds to the green to grey mudstones of the Blue Anchor
97 Formation, and in Northern Ireland to the red and green silty mudstone of the Collin Glen Formation
98 (Mitchell, 2004). Ubiquitously overlying the Mercia Mudstone Group is the relatively thin Penarth
99 Group. Most of the SSDs from SW England, South Wales and Northern Ireland are confined to the
100 Penarth Group (Rhaetian, Late Triassic), which is the primary focus of this study. The Penarth Group
101 can in most instances be subdivided into the Westbury Formation and the overlying Lilstock
102 Formation (Cotham Member and overlying Langport Member, Figure 1B).

103 The Westbury Formation comprises dark-grey, silty, laminated mudstone and sandstones with
 104 current and wave ripples. It has yielded bioclastic accumulations of bivalve fragments, fish bones of
 105 marine and semi-aquatic origin and locally few terrestrial vertebrate remains (Ivimey-Cook, 1974;
 106 Storrs, 1994; Radley and Carpenter, 1998; Swift and Martill, 1999). It is interpreted to be deposited in
 107 lagoonal to shallow marine environments (Hesselbo et al., 2004). In the Severn Estuary area (Bristol
 108 Channel Basin), the top of the Westbury Formation is more clay rich. It is intercalated with nodular
 109 muddy or shelly limestone and sandstones (Richardson, 1911; Radley and Carpenter, 1998). The
 110 overlying Lilstock Formation is divided into two constituent members. At its base, the Cotham
 111 Member corresponds to silty-sandy laminated grey-green mudstones with wave ripples. It has been
 112 interpreted as a coastal, shallow marine to freshwater lagoon environment (Mayall, 1983; Radley and
 113 Swift, 2002; Gallois, 2009). In the Bristol Channel area, a distinctive level of so-called desiccation
 114 cracks with *per-descensum* clastic dykes separates the lower Cotham Member from the upper
 115 Cotham Member (Ivimey-Cook, 1974; Mayall, 1983; Hesselbo et al., 2002; Gallois, 2009). A similar
 116 horizon was recognised by Simms (2003, 2007 and Simms and Jeram, 2007) from the Waterloo
 117 section in Northern Ireland. Although it may correlate with the horizon in SW Great Britain, it sits at a
 118 higher stratigraphic level in the Cotham Member (Jeram et al., this volume). **These cracks have been**
 119 **recently re-interpreted as subaqueous sedimentary (so-called syneresis) cracks (Jeram et al., this**
 120 **volume).** The upper part of the Cotham Member marks a clear enrichment in sand at all localities. At
 121 the top of the Penarth Group, the Langport Member is usually a blue grey to very light grey
 122 mudstone and limestone unit. In SW England, where the very light grey micritic limestones are more
 123 common, they have alternatively been referred to as the White Lias. In SW England, the Langport
 124 Member is also associated with numerous gravitational transport process (Hallam, 1960; Wignall,
 125 2001; Hesselbo et al., 2004). It is particularly well-developed on the South Devon coast where it is
 126 around eight metres thick. The member is restricted to a few decimetre-thick beds in the Severn
 127 Estuary area but in Northern Ireland it is between 4.92 m and 9.27 m thick (Raine et al., this volume).
 128 These deposits correspond to lagoonal to fully marine conditions (Richardson, 1911; Swift, 1995).
 129 Across much of southern Great Britain, the Langport Member is capped by a layer penetrated by
 130 *Diplocraterion* burrows indicating erosion and sediment-starvation in a bed referred to as the “Sun
 131 Bed” (Wignall, 2001; Radley and Swift, 2002; Hesselbo et al., 2004). Finally, the succeeding dark-grey
 132 mudstone–limestone alternations of the Blue Lias Formation in Great Britain and the mudstone
 133 dominated Waterloo Mudstone Formation in Northern Ireland (Hettangian, Early Jurassic) attest to a
 134 deeper marine environment (Deconinck et al., 2003; Gallois, 2007). The stratigraphical nomenclature
 135 used in our logged sections are those used by Mitchell (2004) for Northern Ireland, and by
 136 Warrington et al. (1980) for SW Great Britain.

137 **3. Methods and data**

138 Seven outcrops and four boreholes spanning Late Triassic – Early Jurassic strata were studied across
139 Northern Ireland and Great Britain (Figure 1A). They encompass several Permo-Triassic basins: the
140 Larne and Lough Foyle basins in Northern Ireland and the Wessex and Bristol Channel basins in the
141 south and south west of Great Britain. Outcrop observations were supplemented by analysis of four
142 cores drilled in Northern Ireland in the Larne Basin (Carnduff-1 and Carnduff-2) and in the Lough
143 Foyle Basin (NIRE 05/08-0002 and NIRE 05/08-0003) (Figure 1A).

144 The eleven selected cores and outcrop sections were logged in detail to identify the lithological units
145 and the sedimentary features. In all cores and sections, we observed deformation of the beds at
146 various scales (SSDs), from convolute bedding, mesoscale folds, slumps, micro- and meso-scale faults,
147 and small and large bodies of injected liquefied sediments. In some cases, the upward movement of
148 the liquefied sediments resulted in elongated domes drawn by the upper limit of the liquefied bed.
149 Data collected on the SSDs include (1) their vertical distribution within the sedimentary pile, (2)
150 orientation (strike and dip) and maximum offset of the faults; (3) direction of fold axis and of their
151 overturning direction and (4) strike of elongated domes. The good quality of the outcrops allowed to
152 collect numerous measurements, so that the direction of the SSDs is accurately constrained in each
153 studied site. Attention was paid to identify lateral variations in the SSD trends in each level and
154 variations from one bed to another within a section. Orientation data include 360 measurements in
155 Pinhay Bay, 31 measurements in Lavernock, 34 measurements in Lilstock, 31 measurements in Saint
156 Audrie's Bay, 91 measurements in Waterloo Bay. No direction data could be obtained in the
157 Northern Ireland cores because they were not oriented. These data together allow to characterize
158 the recurrence and style of deformation in relation with the lithology and to obtain a statistically
159 representative determination of the SSD orientations.

160

161 **4. Results: distribution and directional characterisation of SSD in Triassic–Jurassic boundary**

162 **strata**4.1 *Northern Ireland (Larne and Lough Foyle basins)*

163 4.1.1 *Distribution of SSDs*

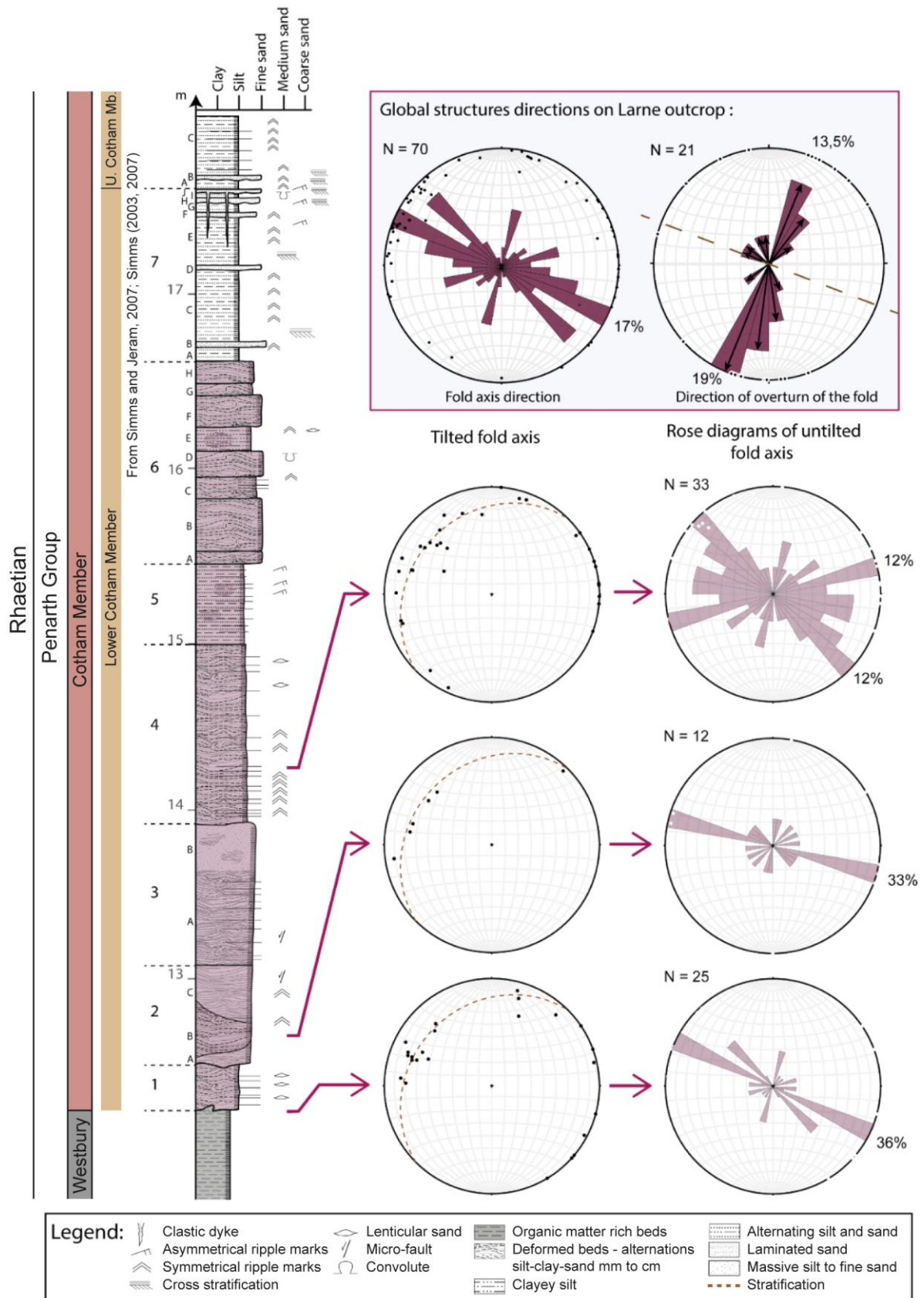
164 On the Waterloo Bay foreshore section at Larne, the Westbury Formation corresponds to dark grey
165 laminated clays with occasional silty to sandy laminated layers (Figs. 2 and 3). The boundary between
166 the Westbury Formation and the Cotham Member is deformed by centimetre- to decimetre-scale
167 dome structures (Figs. 2 and 3B). This is particularly visible in the western part of the outcrop. The
168 SSDs affect units 1 to 6H (Fig. 2). Dark grey mudstone of the upper Westbury Formation is injected

169 throughout the overlying coarser sediments of the Cotham Member, which pinch out against the
170 dome walls. Claystone and sandstone alternations of the basal Cotham Member are deformed
171 around these injections and form folds caused by the upward movement of the clay. These
172 deformations include diapirs and anticlinal cusps corresponding to fluid escape from overpressured
173 clay up through the non-indurated sandy alternations (Ghosh et al., 2012). The lower Cotham
174 Member is furthermore disturbed by numerous centimetre- to metre-scale isoclinal and recumbent
175 folds (Fig. 3C and D). These folds affect laminated millimetre- to centimetre-thick beds of siltstone,
176 sandstone and claystone (units 1 to 6, Figure 2). The larger folds are in the lenticular unit 2B and have
177 a width and height of 1.0–1.5 m. Second-order folds, with shorter wavelength are observed in the
178 sandier intervals (Figure D). Some areas are stretched and others contracted causing boudinage and
179 variations of sandstone layer thickness, which has amplified the shape of existing wave ripples (Fig.
180 3D). The interval with SSDs is 4.6 m in thickness. However, the density of SSDs varies laterally, and
181 less deformed areas can be recognised. Unit 3B corresponds to a finer and more homogeneous
182 siltstone that was less affected by soft deformations. From unit 7 to the top of the section, the layers
183 are undisturbed despite having an overall similar lithology to the underlying deformed units (Fig. 2).
184 Only one level with *per-descensum* centimetre-thick dykes was recognised at the top of unit 7. **These**
185 **dykes show multidirectional orientations and were first recorded by Simms and Jeram (2007). They**
186 **are discussed in detail and interpreted by Jeram et al. (this volume) as two or three generations of**
187 **subaqueous sedimentary (so-called syneresis) cracking, possibly linked to a seismic event.**

188 The Carnduff-1 and Carnduff-2 cores from the Larne Basin are 2.82 and 2.58 km away, respectively,
189 from the Waterloo Bay section at Larne (Fig. 4). The cores display very similar features to those of the
190 outcrop. Thicknesses of the individual lithostratigraphical units are comparable between the cores
191 and the nearby outcrop. SSDs occur in the cores from the base of Cotham Member and comprise a
192 4.3 m thick interval in Carnduff-1 and a 4.4 m thick interval in Carnduff-2 (Figure 4). The layers
193 bearing the SSDs in these cores and in the Waterloo Bay outcrop are easily correlated using marker-
194 beds thanks to their limited geographical separation. The shell-rich levels affected by convolute
195 bedding in the upper Westbury Formation, the three sandy layers at the top of Cotham Member, and
196 the levels rich in bivalve shells at the base of Blue Lias Formation are very good local bed markers
197 (Fig. 4). The deformations observed in Carnduff-1 and Carnduff-2 cores include millimetre- to
198 centimetre-scale recumbent folds, isoclinal folds and convolute bedding. Numerous normal micro-
199 faults with length of several centimetres also affect the upper half of the deformed level. This is well
200 seen in finely laminated deposits that form micro-graben-like structures. Variations in bed thickness
201 are observed on either side of several micro-faults, suggesting that some of them are syndimentary

202 faults. The deposits above the deformed level in the Carnduff-1 core are cut by a centimetre-wide
203 clastic dyke.

204



205

206 Figure 2. Detailed log section of the Waterloo Bay foreshore, Larne. SSDs are observed in units 1 to 6
 207 (beds in purple). Plots on the left correspond to fold axes with the present day dip. Rose diagrams on

208 the right correspond to the direction distribution of folds along the outcrops. Both diagrams at the
209 top give the fold axis distribution for the whole section. N: number of data. Note that all fold axes lie
210 in the bedding plane. Folds thus formed with a sub-horizontal axis before the tilting of beds.

211 The NIRE 05/08-0002 and NIRE 05/08-0003 cores are situated in the Lough Foyle Basin in Co.
212 Londonderry, about 68 km NW from the Waterloo Bay section (Figs. 1 and 4). In the Lough Foyle
213 Basin, the tidal (flaser-bedded) deposits of the Cotham Member are thicker than those of the Larne
214 Basin. The base of the formation is characterised by a massive, apparently un-deformed grey-green
215 silty clay. Elsewhere in the region this grey clay has been recorded as having *Rhaetavicula contorta*, a
216 common bivalve in the Westbury Formation (Bazley et al., 1997). The Cotham Member in the Lough
217 Foyle Basin comprises comparable facies and numerous recumbent and isoclinal folds with similar
218 size to those in the Cotham Member in the Larne Basin, as observed in the Waterloo Bay section and
219 in Carnduff-1 and Carnduff-2 cores. The deformed level in NIRE 05/08-0003 is 5.8 meters in thickness
220 (Fig. 4). Numerous synsedimentary normal micro-faults are observed throughout the sandy layers of
221 the deformed level. In NIRE 05/08-0002, deformations are restricted to a two-metre-thick interval in
222 the upper part of the Cotham Member. However, because of the condition of the core, it cannot be
223 determined whether there are deformations in the lower part. In Northern Ireland, the original
224 laminated internal structure of the deposit is always preserved during the deformation. The
225 widespread occurrence of overturned folds suggests that a shear stress has been applied on the
226 sedimentary material during liquefaction of the sediments.

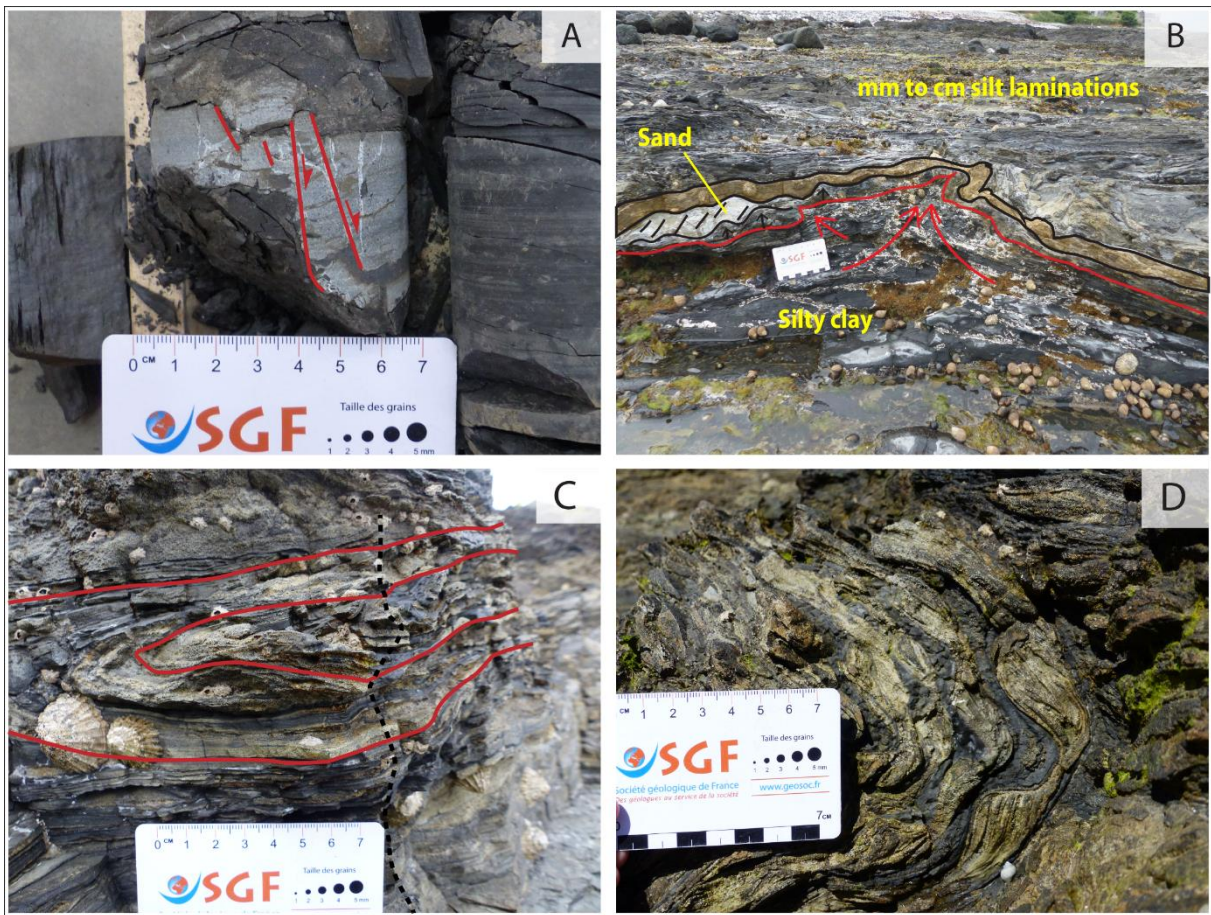
227 To summarise, the same disturbed interval of the lower Cotham Member in Northern Ireland (level 2,
228 Fig. 4) can be correlated between the 5 sections throughout the two basins.

229 In addition to this main deformed layer in the Cotham Member, the base of the Westbury Formation
230 is also affected by soft deformations in the NIRE 05/08-0002 and NIRE 05/08-0003 cores (Fig. 4). The
231 thickness of these deformed levels (level 1, Fig. 4) is respectively 2.5 and 1.0 m. Within those two
232 cores, the deformations are especially well-observed in a 15 to 20 cm thick interval made of clay and
233 sand laminae. Some of the centimetre-scale folds, convolute bedding, sandstone boudins and
234 angular undeformed clasts may result from bioturbation. However, the occurrence of several
235 millimetric to centimetric normal faults and graben structures throughout the two cores in the
236 Westbury Formation indicates that the deformations are most likely non-biological in origin (Fig. 3A).
237 Thickness variations from either side of the observed micro-faults also indicate syn-sedimentary
238 activity during the deposition of the Westbury Formation.

239 Sand- and shell-rich levels disturbed by convolute bedding and synsedimentary faults of millimetre-
240 to centimetre displacement in the Westbury Formation are interpreted as a moderate deformation

241 event (level 1, Figure 4) that affected the Westbury Formation in the Lough Foyle Basin. In our
242 studied sites in the Larne Basin, some convolute bedded shelly levels with burrows are found at the
243 top of the Westbury Formation (Fig. 4), and are likely to equate to this deformation event, as other
244 SSDs have been found in the upper half of the Westbury Fm. in Cloghfin Port, South of Islandmagee
245 (Jeram, et al. this volume). However, the absence of normal faults and of typical liquefaction
246 structures does not rule out the the possibility of a bioturbation origin.

247

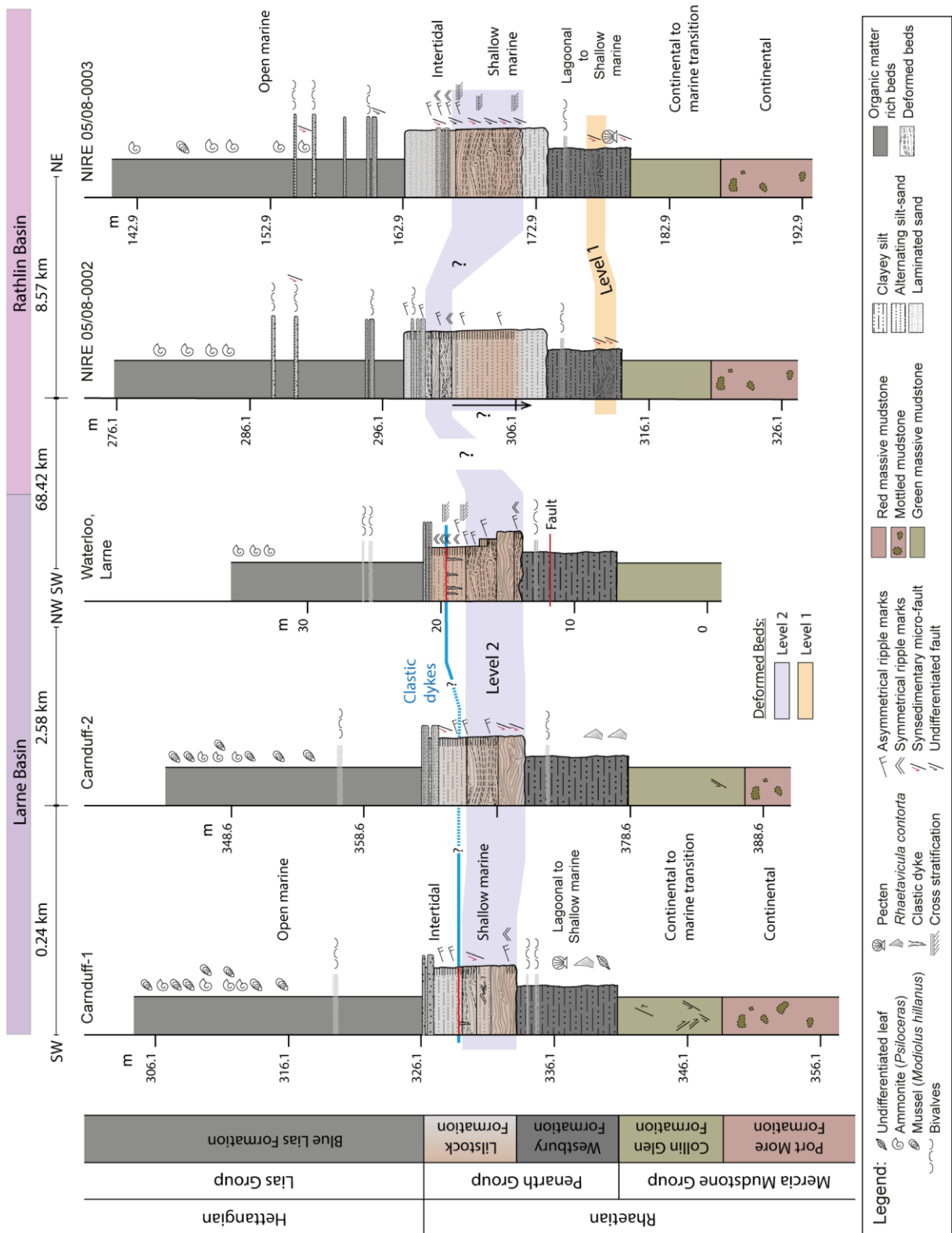


248
249 Figure 3. SSDs observed in Northern Ireland. (A) Synsedimentary micro-faults in the Westbury
250 Formation, NIRE 05/08-0003 core. (B) Diapir injection structure at the boundary between the
251 Westbury Formation and the Cotham Member, Waterloo Bay. (C) Recumbent fold in the lower
252 Cotham Member, Waterloo Bay. (D) Second generation of folds and boudinage in a larger fold,
253 Waterloo Bay.

254

255

256



257

258 Figure 4: Log sections and position of deformed layers in Northern Ireland. Carnduff-1, Carnduff-2,
 259 NIRE 05/08-0002 and NIRE 05/08-0003 correspond to cores, and the Waterloo, Larne, corresponds to
 260 the outcrop in Waterloo Bay foreshore.

261 4.1.2 Directional characterisation of the SSDs (Waterloo Bay foreshore, Larne Basin)

262 The excellent outcrop at the Waterloo Bay foreshore exposure in Northern Ireland, allows the SSD
263 direction of the SSDs to be studied. At the boundary between the Westbury Formation and the
264 overlying Cotham Member, the elongation of the diapirs show a clear preferred N120°E orientation,
265 accounting for 36% of the 25 measured injections (Fig. 2). In unit 2B, various fold orientations have
266 been observed but a large proportion (33% of 12 measurements) show a roughly similar (N110°E)
267 trend. Fold directions are more scattered in unit 4 where two main directions are recognised: 12%
268 have a N130°E direction, similar to that observed in underlying layers and 12% have a N70°E
269 direction from 33 measurements. These results highlight a mean NW–SE fold axis direction through
270 the deformed levels. The overturned directions of the folds are either oriented toward the North or
271 toward the South. This likely excludes sliding along local submarine slopes as a control of the
272 observed soft-sediment folding. On the other hand, the constant orientation of the strain ellipse
273 suggests a tectonic origin of the deformation structures that were thus controlled by the local state
274 of stresses.

275 *4.2 Bristol Channel Basin*

276 *4.2.1 Distribution of SSDs*

277

278 In the Bristol Channel Basin, the Cotham Member corresponds to a calcareous mudstone with
279 millimetre- to centimetre-scale siltstone and fine sandstone laminations. The lithology is substantially
280 similar to Northern Ireland, with a more prevalent carbonate component. Six stratigraphic intervals
281 have been defined at St Mary's Well Bay, eight at Lavernock Point, five at Lilstock, and five at St
282 Audrie's Bay (Fig. 5). Lithofacies correlations using marker beds such as dyked horizons appear
283 obvious between the four sections (Fig. 5). The boundary between the Westbury Formation and the
284 Cotham Member is not affected by diapiric injections as in the Larne Basin. However, at Lavernock
285 Point, recumbent folds involving pockets of dark organic-rich material with bioclasts that have
286 originated from the underlying Westbury Formation are present in the first 70 cm of the Cotham
287 Member (Figure 5, bed 2A, and Fig. 6A). Reworked bivalves were recorded in the region in the basal
288 beds of the Cotham Member by Waters and Lawrence (1987).

289 At St Mary's Well Bay, South Wales, and St Audrie's Bay, Somerset, the lower Cotham Member is also
290 affected by numerous recumbent and isoclinal folds (Figure 5 and Figure 6C). At Lilstock, two distinct
291 levels of deformation (N1 and N2, Fig.5) within the lower Cotham Member can be followed along the
292 cliff and on the foreshore. The Lilstock section shows many overturned and recumbent folds in unit
293 2C (in the middle of the member) and in unit 2E (Figure 5 and Figure 6B). The two liquefied levels are
294 here separated by an un-deformed 60 cm thick mudstone with beds of siltstone and fine sandstone
295 (unit 2D).

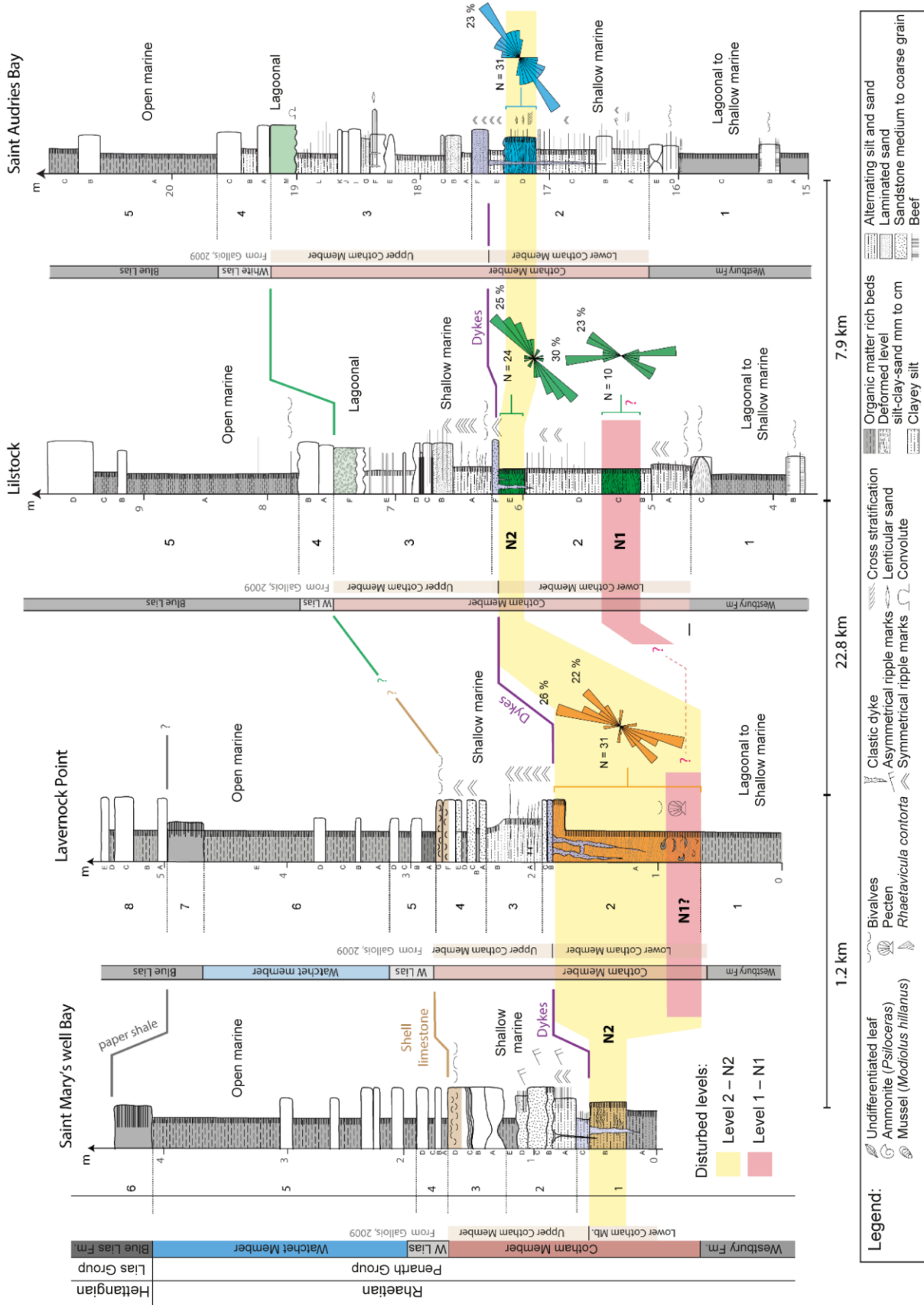
296 At St Audrie's Bay, St Mary's Well Bay and Lavernock Point, deformations are systematically located
297 below the level of polygonal dykes (Fig. 5). At Lavernock point, the thickness of the disturbed interval
298 is greater than at any other localities.

299 4.2.2 Directional characterisation of SSDs

300 Ninety-six fold axes have been measured in the deformed levels of the Cotham Member in the Bristol
301 Channel area (Figure . 5). Thirty-one folds were measured at each St Audrie's Bay and Lavernock
302 Point sections, and 34 folds at Lilstock. At St Mary's Well Bay, the observation conditions of the cliff
303 are insufficient to measure enough fold structures.

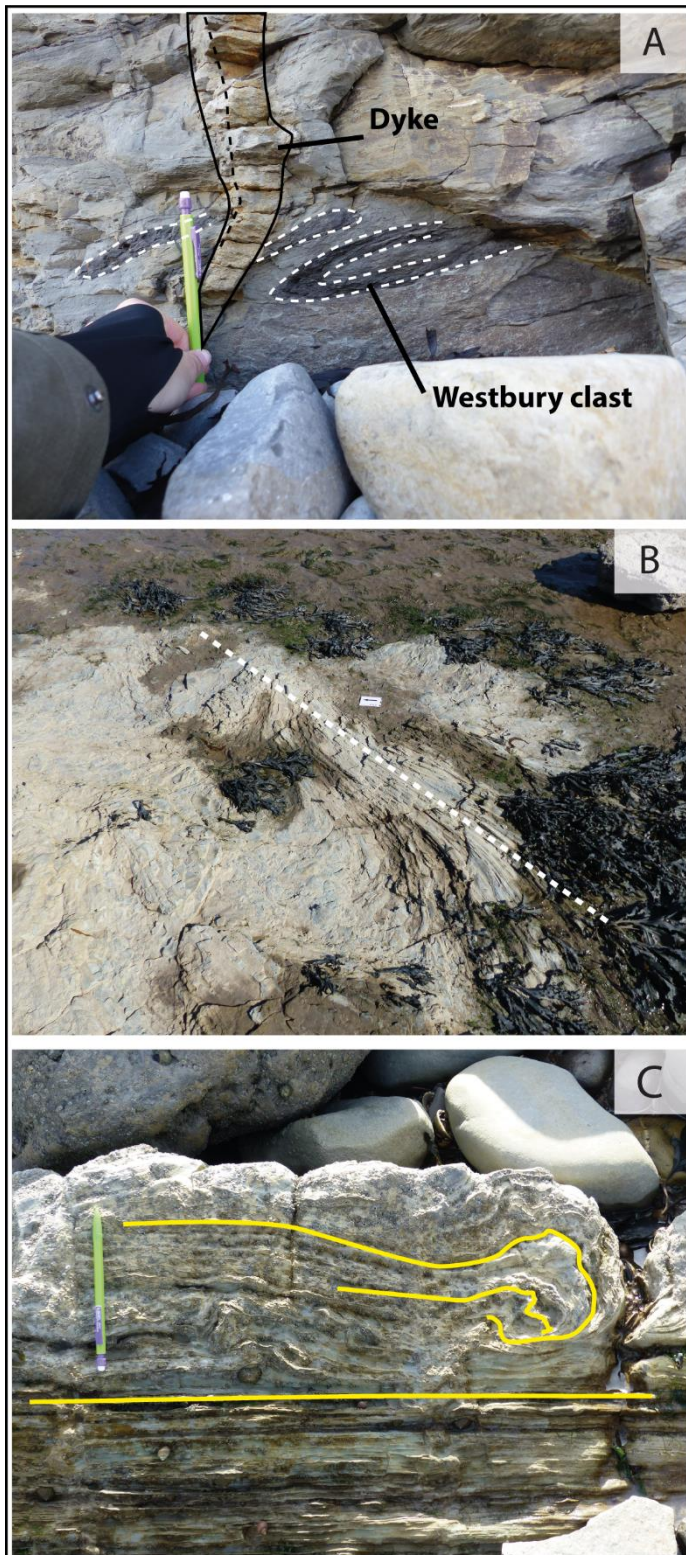
304 At St Audrie's Bay, deformations only occur in the 40 cm thick unit 2D, situated just below the layer
305 that fed the clastic dykes. Despite a moderate dispersion of the data, a preferred NE–SW fold axis
306 direction, which represent 23% of the data, is recognised in the uppermost part of the lower Cotham
307 Member. This is in agreement with the results from Northern Ireland, according to which all
308 deformations in a given level were governed by anisotropic stresses. Accordingly, folds in the 20 cm

309 thick unit 2E at Lilstock have the same preferred NE–SW trend (25% of the data). Within the
310 underlying deformed unit 2C, the fold axes show two directions: a main N–S direction (30% of the
311 data) and a secondary NNE–SSW direction (23% of the data). At Lavernock Point, the fold axes
312 observed within the deformed beds of the lower Cotham Member which are here 70 cm thick also
313 show two main directions. A first NE–SW direction (26% of the data, Fig. 5) correspond to the one
314 observed at St Audrie’s Bay and in unit 2E at Lilstock. A second NNE–SSW direction (22% of the data)
315 is quite similar to the orientation of the folds within unit 2C at Lilstock.



317 Figure 5. Logged sections and lithostratigraphic correlations within the Bristol Channel area. Rose
318 diagrams correspond to the main direction axis of folds for each deformed level. Values of the main
319 peaks are indicated in percentage. N: number of data.

320



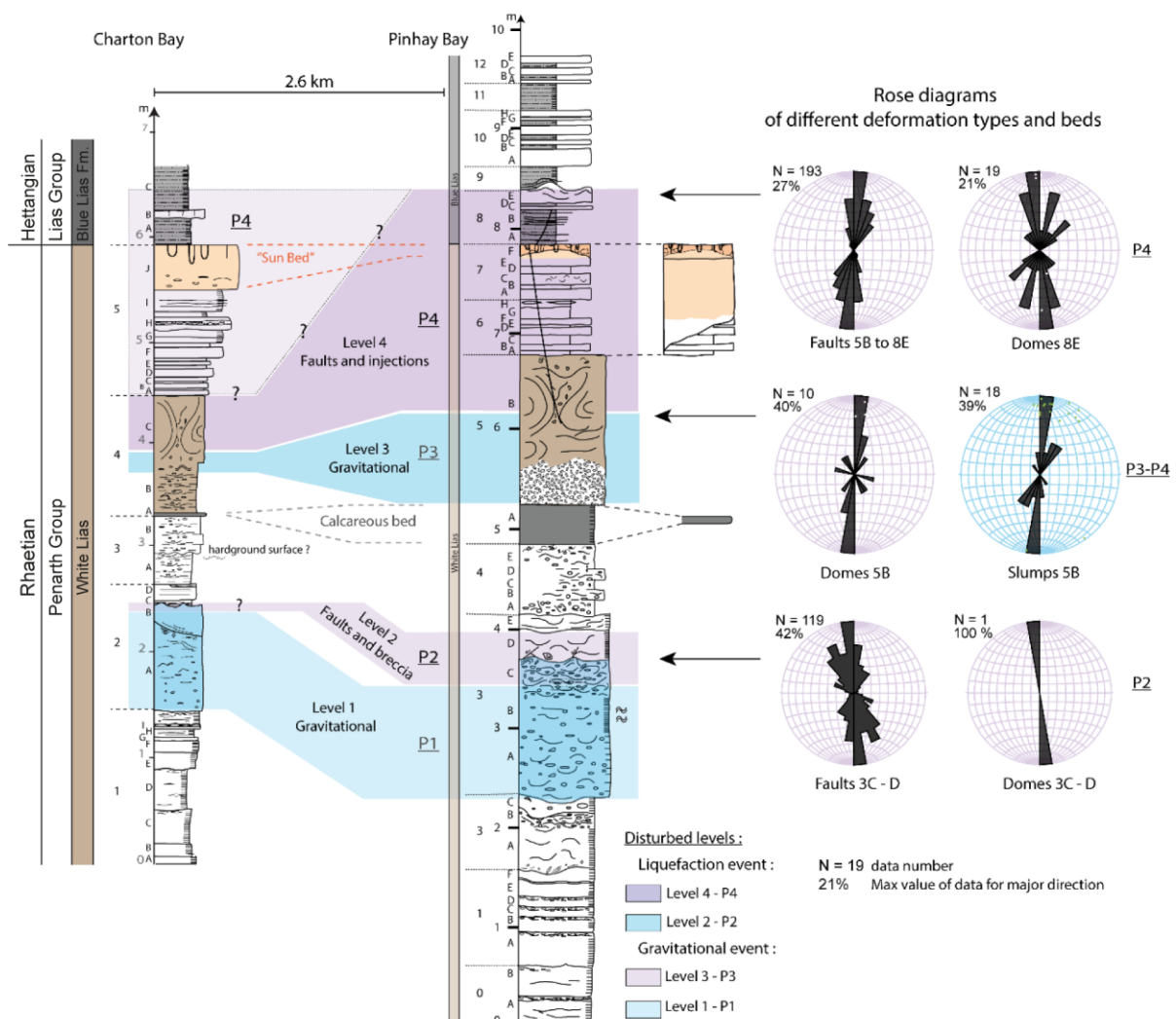
321
322 Figure 6. SSDs in SW Great Britain (Bristol Channel Basin). (A) Deformed clast of the Westbury
323 Formation within the base of the lower Cotham Member at Lavernock Point (unit 2A). The clastic
324 dyke postdates the recumbent fold formation. (B) Isoclinal fold axis in the lower Cotham Member on
325 the foreshore (unit 2E), Lilstock. (C) Recumbent fold in the lower Cotham Member (unit 2D) at St
326 Audrie's Bay.

327

328 4.3 South Devon Coast (Wessex Basin)

329 4.3.1 Distribution of SSDs

330 At Charton Bay and Pinhay Bay, South Devon, the “White Lias” facies of the Langport Member is
 331 more developed than in the Bristol Channel area and corresponds to micritic limestones. It is affected
 332 by many SSDs of various types and scales. Six sedimentary units and twelve sedimentary units have
 333 been distinguished at the Charton Bay and Pinhay Bay sections, respectively (Fig. 7). Two major
 334 deformed levels (levels 2 and 4, in pink color in Fig. 7) have been recognised in both localities.



335

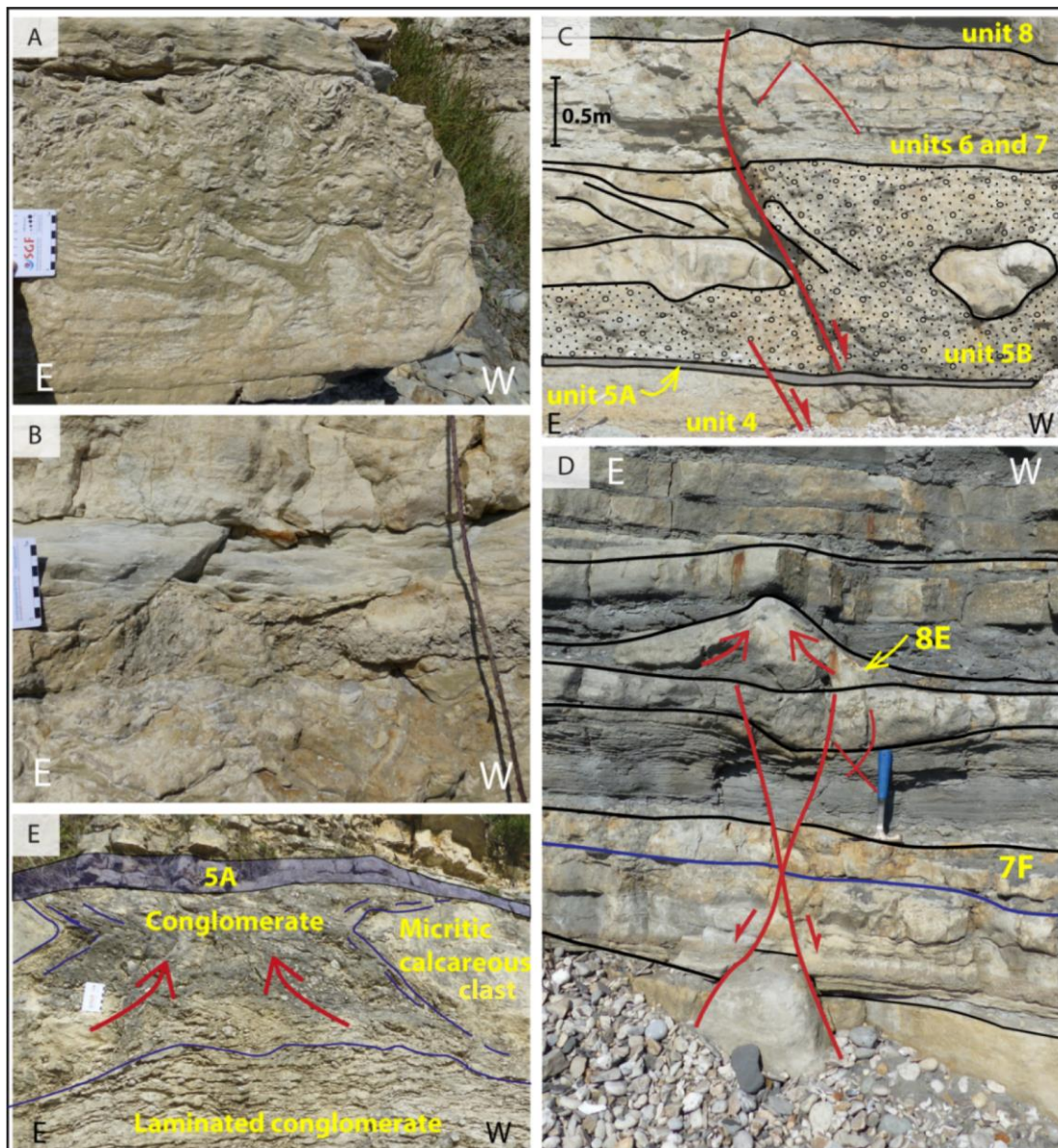
336 Figure 7. Logged sections and position of deformed levels of the South Devon coast area. Rose
 337 diagrams correspond to the main direction of folds, faults and domes, for each deformed level at
 338 Pinhay Bay.

339 Units 2A and 2B at Charton Bay and 3A and 3B at Pinhay Bay, correspond to debris flow deposits.
340 They are respectively 1.00 m and 1.85 m thick (level 1, Figure 7) and are composed of a monogenic
341 calcareous muddy conglomerate with an erosive base and an inverse to undefined grading. At Pinhay
342 Bay, the upper part of this level is affected by numerous decimetre-scale convolute beds in unit 3B,
343 which result from important fluid escape features (Figure 8A).

344
345 At Pinhay Bay, unit 3C, just above the debris flow deposit, is almost entirely brecciated. The 3C–3D
346 boundary is affected by small normal faults being about 50 cm in length and having an up to 10
347 centimetres net slip (level 2, Fig. 7 and Figure 8B). The syn-sedimentary character of those faults is
348 suggested by bed thickness variations between the footwall and hangingwall. Within unit 3C,
349 liquefied material have been molded along the faults as injective domes and peaks. The location and
350 shape of the injective bodies seem to be clearly controlled by faults. It suggests that the normal faults
351 guided the upward injections. This deformation required a semi-indurated material to allow brittle
352 deformation, brecciation and liquefaction of the sediment. No faults have been observed at Charton
353 Bay, only some rare fluid escape features were observed at the top of unit 2B (Figure 7).

354
355 At Pinhay Bay, unit 5B corresponds to a 1.50 m thick disturbed interval. The base of the bed is
356 completely brecciated and corresponds to an accumulation of angular clasts (level 3, Figure 7). The
357 outcrop is also affected by several metre-scale normal faults, which cut units 5B to 8E (level 4, Fig. 7).
358 To the east, unit 5B is totally disorganised and some metre-scale ball-shaped elements are preserved
359 in the middle part of the layer. As for units 3C and 3D, the faults that affected unit 5B clearly delimit
360 the preserved versus liquefied zones. The injective domes are molded along the faults, which appear
361 to have been at the same time a guide for vertical movement of the liquefied sediment and a
362 horizontal barrier to deformation (Figure 8C). In the western part of the section, the faults are less
363 prominent and the initial deposit of unit 5B is partially preserved. The initial structure of unit 5B
364 corresponds to a slumped decimetre-scale package of beds. Units 6 and 7 are preserved, but have
365 faults cutting across them. Unit 8E shows the occurrence of a series of injective domes or bulges with
366 an upward domed shape. These features are all observed at the top of normal faults (Figure 8D).
367 They indicate the local liquefaction and upward flow of the soft sediment material caused by the
368 displacement along the underlying normal faults. These faults have affected the sedimentary pile up
369 to unit 8E. The injections have also deformed the overlying bed.

370



371
 372 Figure 8. SSDs observed in South Devon (A) Fluid escapes features highlighted by convolute bedding
 373 at the top of a debris flow, unit 3A, Pinhay Bay. (B) Synsedimentary fault between units 3C and 3D at
 374 Pinhay Bay. Unit 3C is injected along the fault and forms a dome structure. (C) Normal fault affecting
 375 units 5B to 8E at Pinhay Bay. The fault limits the liquefaction of the slumped unit 5B (shown by
 376 stippled pattern). (D) Normal fault with injection feature at the top of unit 8E. (E) Massive injection
 377 features within a matrix-supported conglomerate throughout unit 4C at Charton Bay. Unit 5A is not
 378 affected (marked by coloured overlay).

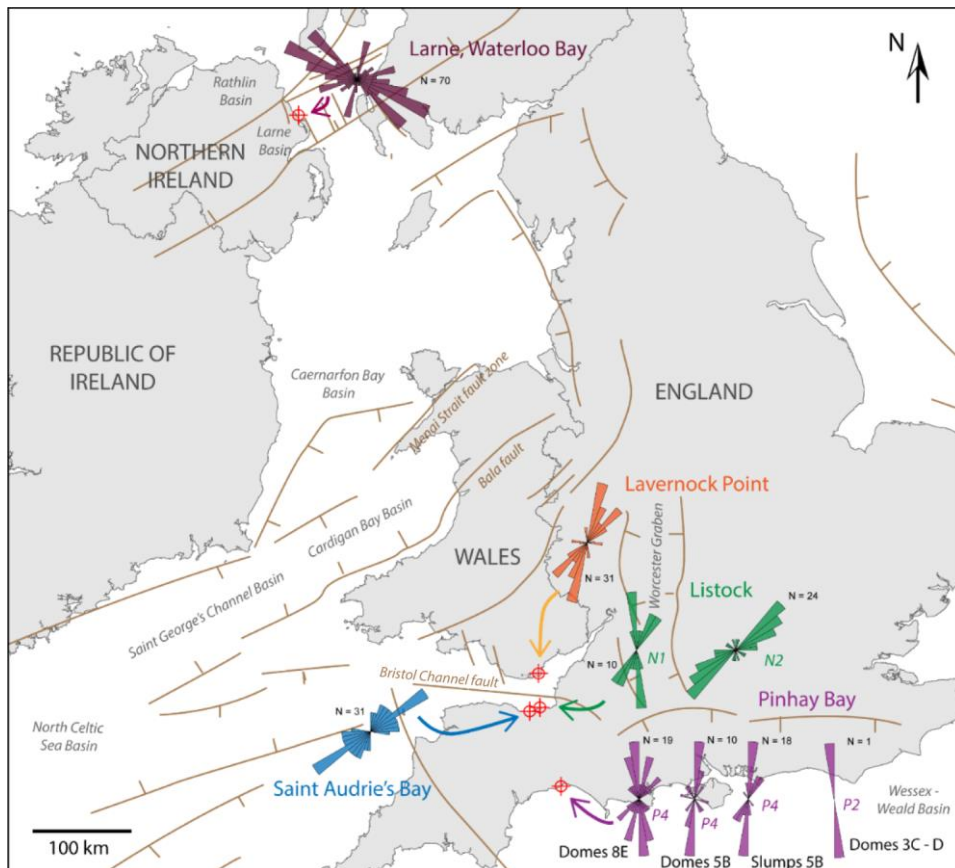
379 At Charton Bay, the unit 4C is a liquefied slumped bed that is similar to unit 5B at Pinhay Bay (level 4,
 380 Figure 7). This unit is cut and partially deformed by injections from the underlying beds. It
 381 corresponds to a micritic limestone affected by numerous fluid escape structures at its base (e.g.
 382 convolute bedding). The original sediment structure is partially disorganised at the top of the bed.
 383 Unlike at Pinhay Bay, this interval is not affected by faulting and does not show any dome-like
 384 injection features directly associated with the faults.

385

386 4.3.2 Directional characterisation of SSDs

387 A statistical study has been carried out on the measurements performed on all types of SSDs axes
388 from Pinhay Bay. The data include the axis directions of the elongation of injective domes of units 3C
389 (1 measurement), 5B (10 measurements), 8E (19 measurements), and the axis of the slump in unit 5B
390 (18 measurements). The orientations of the normal faults affecting units 3C to 3D (119
391 measurements) and 5E to 8E (193 measurements) were also measured and included in the statistical
392 analyses (Figure 7).

393 Both fault sets in units 3C/3D and 5B to 8E have a common N–S to NNE–SSW orientation
394 (respectively 42% and 27%). These faults show dips towards the east as well as towards the west. The
395 injective domes in units 3C and 5B, and the helmet-like domes in unit 8E located at the fault tips
396 show a similar N–S to NNE–SSW direction (respectively 100%, 40% and 21%). Finally, slumps
397 measured in unit 5B also show a main N–S axis (39%) with a subordinate NNE–SSW orientation. To
398 summarise, the major directions of structures from each site studied in the UK are shown in the
399 Figure .



400

401 Figure 9. Main orientations of deformation structures observed in each outcrop in the UK. N: number
 402 of data. N1 and N2 in Lilstock, P2 and P4 in Pinhay Bay refer to the two deformed levels recognised in
 403 these sites.

404

405

406

407

408 5. Discussion

409 5.1 A seismic origin for Rhaetian SSDs in the UK

410 All observed SSDs occurs in a limited stratigraphic interval at the Triassic–Jurassic boundary in SW
 411 England, S Wales and Northern Ireland. These SSDs have been observed in four distinct areas over a
 412 distance of more than 1000 km, namely the Lough Foyle and Larne basins in Northern Ireland, the
 413 Bristol Channel Basin in the Severn Estuary area (S Wales and N Somerset Coast) and the Wessex
 414 Basin on the South Devon coast in SW England. **In northern Ireland, in coastal sections to the south of**
 415 **Waterloo Bay, Jeram et al. (this volume) also described SSDs in the Westbury Fm. at Cloghfin Port,**

416 Islandmagee and in the Lower Cothan Member at Cloghan Point, Whitehead. In addition, SSDs have
417 been previously documented in other areas of the UK, namely in Central England and North Wales
418 (Simms, 2007). This spatial distribution suggests a common and large regional extent causal link.

419 Direct or indirect field evidences of earthquake(s) as a trigger of SSDs in the study sites include:

420 (1) All major SSDs and related fluid-escape features being directly molded on and associated with
421 metric to plurimetric in length normal faults at Pinhay Bay, showing a clear genetic relationship
422 linking SSDs with faults;

423 (2) Faults axes and dome axes of SSDs measured in the field having a similar N–S to NNE–SSW
424 direction at Pinhay Bay, again suggesting that SSD distributions were driven by faults activity;

425 (3) The directions of deformation being homogeneous for each disturbed level in all study sites,
426 suggesting a unique SSD trigger for a given disturbed level;

427 (4) The deformation structures having very well constrained orientations when comparing different
428 sites (e.g., the N–S to NE–SW directions in south England, Fig. 9), regardless of the deformation type
429 observed: only earthquake(s) as a trigger may have induced such a (multi-) regional consistency in
430 SSDs orientations;

431 (5) Numerous laminae thickness variations being observed from either sides of small-scale (up to
432 several centimetres in length) syn-sedimentary normal micro-faults in Carnduff-1 and Carnduff-2
433 cores from the Larne Basin, showing the activity of syn-sedimentary micro-faults;

434 (6) The opposite overturning directions of the folds being either oriented towards the north or the
435 south in the Waterloo Bay foreshore outcrop (Larne Basin) and faults dipping towards the east and
436 towards the west at Pinhay Bay (Wessex Basin) without preferential orientation. This rules out that
437 local gravity sliding along slopes is a unique potential trigger of SSD formation;

438 None of the potential other triggers of SSDs such as tsunamis (Takashimizu and Masuda, 2000;
439 Nanayama et al., 2000; Schnyder et al., 2005; Le Roux et al., 2008), tidal flux and tidal bores (Tessier
440 and Terwindt, 1994; Greb and Archer, 2007), storm waves and breaking waves (Molina et al., 1998)
441 or rapid sedimentation and loading may explain the direct link observed between SSD and faults
442 (Pinhay Bay and Larne Basin) and the consistent directions of SSDs at a regional scale in various sites
443 (e.g., Southern England). As a matter of fact, tidal flux and tidal bores, storm waves, breaking waves
444 and loading features have no genetic link(s) to fault patterns. They have commonly local effects and
445 usually do not show inter-regional common directions of structures for various basins, as observed in

446 our study. We do not favor a bolide impact-related tsunami hypothesis to explain the observed SSDs
447 distribution, because we commonly observed various SSDs axis directions in different stratigraphic
448 levels. This exclude a unique deformation event, otherwise SSDs should have a unique trend.
449 Moreover, differences in the fault size in the two deformed levels at Pinhay is also in agreement of
450 successive shearing events with different intensity. Additional investigations in Northern Ireland by
451 Jeram et al. (this volume) evidence SSDs occurrence immediately adjacent to faults in the Westbury
452 Fm at Cloghfin Port and increasing SSDs intensity towards a local fault, directly pointing to a seismic
453 origin of those SSDs.

454 In addition, the large-scale extensional context in north-western Europe during the Triassic and early
455 Jurassic (Ziegler and Stampfli, 2001; Ziegler and Dezes, 2006) may certainly have triggered numerous
456 earthquakes, leading to a context which may have possibly formed earthquakes-induced SSDs.

457 All these observations support a seismic cause as the origin of the liquefaction and the formation of
458 the disturbed levels. We thus propose that the liquefaction and deformation of the Penarth Group
459 deposits was due to the activity of local faults during or shortly after sediment deposition, as
460 suggested by Mayall (1983) and as highlighted by Jeram et al. (this volume) for Northern Ireland
461 sites.

462 *5.2 Role of lithology and fluids in the style of deformation and SSDs localisation*

463 *5.2.1 Relation between SSDs type and lithology*

464 Relatively fine-grained sediments like siltstones to fine sandstones and showing a strong vertical
465 grain size contrast are known to be prone to SSDs formation after suffering an initial shock,
466 whatever its origin (Lowe, 1975; Allen, 1982; Montenat et al, 2007). Therefore, in all our study sites,
467 the fine-grained, alternating lithology, was certainly favourable for SSDs formation. We show that
468 lithological heterogeneity is also important at various scales, as we observed a role on SSDs
469 formation for a millimetric to centrimetric lamination of the sedimentary pile (Bristol Channel and
470 Northern Ireland) and pluri- metric bedding lithological contrasts (Devon).

471 However, differences arise when comparing the style of deformation and its location in the
472 sedimentary pile in our study sites. In the Bristol Channel and in Northern Ireland, only small normal
473 faults of centimetre size coexist with recumbent and isoclinal folds of millimetric to metric
474 dimensions. The original laminations largely remained coherent. On the contrary, in Devon, the
475 disturbed layers present metre-scale injections and fluid escape features and highly disturbed,
476 intensely homogenised intervals. Those two different deformations types in the Bristol Channel and

477 in Northern Ireland compared to Pinhay Bay in Devon is probably explained, at least partly, by the
478 contrasting mechanical properties of the two lithofacies, with a greater carbonate content at Pinhay
479 Bay than at other sites. Higher carbonate composition at Pinhay Bay may have caused a faster
480 induration of the depositional mud shortly after deposition, allowing brittle failure of the hardened
481 sediments after the earthquake shock. The immediately following liquefaction then induced a re-
482 mobilization of a thick sedimentary pile. On the contrary, in the Bristol Channel and in Northern
483 Ireland, siliciclastic beds with clay intervals promoted a more ductile behavior and the deformation
484 was restricted to a rather thin sedimentary pile.

485 In even greater detail, one can observed subtle differences in SSDs style that were probably linked to
486 lithology. The deformed sediments of Northern Ireland correspond to finely laminated silty-sandy
487 mudstones, slightly coarser, when compared with the ones deformed around the Bristol Channel
488 Basin. Furthermore, the thickness of the deformed layer (up to 4.5 m) and the size of SSDs are also
489 greater in Northern Ireland than in the Bristol Channel Basin. Usual thicknesses of liquefied levels
490 reported in the literature (Allen, 1977; Plaziat and Ahmamou, 1998; Ken-Tor et al., 2001; Greb and
491 Archer, 2007) range from a few centimetres to one metre, which highlights the intensity of
492 deformation in Northern Ireland. The greater susceptibility of silty/sandy materials to liquefaction
493 (when alternating with more impermeable layers) may be at the origin of the increase in the size of
494 the folds in Northern Ireland (Obermeier, 1996) and their higher deformed level thicknesses,
495 **although it has been suggested that the reduced thickness of the SSDs Unit in the Bristol Channel**
496 **Basin was due to a subsequent erosion, as evidenced by an erosion surface that truncates some of**
497 **the SSDs (Simms, 2003, 2007).**

498

499 *5.2.2 Role of fluids, faulting and overpressure*

500 In the Pinhay Bay section, active faults played a key role in the localisation of deformation in the
501 beds. As stressed above, the liquefaction and associated SSDs are often localized at the top of faults
502 (Figs. 7 and 8). On the other hand, the faults also locally played a mechanical barrier role in the
503 lateral propagation of deformation. As an example, in unit 5B at Pinhay Bay, only the hangingwall of
504 faults is totally liquefied and de-structured (Fig. 8C), suggesting the occurrence of such a mechanical
505 barrier role that inhibited the lateral extension of deformation. An additional interesting observation
506 at Pihnay Bay is that the liquefaction guided by faults only re-mobilise some specific levels, namely
507 the coarse, brecciated, slumps-rich levels, and not the finer, more homogeneous beds (Fig. 7). The
508 important incorporation of water during these major gravity events probably facilitated the

509 overpressure of the interstitial water during liquefaction phenomena and led to the brecciation and
510 then the homogenisation of the initial deposit. Thus, the high porosity and the pre-earthquake(s)
511 residual water content of these sedimentary units made them very sensitive to the phenomenon of
512 liquefaction and localized almost all of the deformation. The overlying marl package of the Waterloo
513 Mudstone Formation in Northern Ireland and the Blue Lias Formation in the Devon may have
514 enhanced the overpressure processes, helping to concentrate the deformation on the topmost part
515 of the underlying Penarth Group.

516

517 *5.3 Comparing the SSDs and active faults at the Triassic-Jurassic boundary in the UK*

518 One major trend of deformation emerges clearly for each of the study locations, and often
519 corresponds to the direction of local fault(s) (Figure). In Northern Ireland, the major NW–SE
520 direction observed at Waterloo Bay, Larne is relatively similar to the trend of Permo-Triassic basin-
521 bounding faults which have a NNW–SSE trend (Ruffell and Shelton, 1999). The second and minor
522 orientation found in those sites, well developed at the top of the disturbed level is equivalent to the
523 ENE–WSW trending Caledonian fault trend (Anderson et al. 1995; Holdsworth et al., 2012). In the
524 Bristol Channel area, the major N–S or NE–SW direction identified by the SSDs, **in accordance with**
525 **previous limited results from Simms (2003, 2007)**, is similar to the general orientation of the Cardigan
526 Bay and Caernarfon basins at the NW of the Bristol Channel (Dobson et al., 1982; Tappin, 1994).
527 These neighbouring basins are bordered by NE–SW Caledonian faults that were reactivated during
528 the first opening during Permian and Triassic times, such as the Bala Fault or Menai Straits Fault Zone
529 (Dobson et al., 1982; Tappin, 1994; Coward, 1995). The N–S trending faults bounding the more distal
530 Worcester Graben (Fig. 9), may have also been involved in SSDs formation in the Bristol Channel
531 Basin. The Worcester Basin is bordered by inherited Variscan normal faults (Holdsworth et al., 2012),
532 but this basin shows a low subsidence during the end of the Triassic (Whittaker, 1985). The known
533 NE–SW extension direction of the Bristol Channel Basin defined by structural analysis during the
534 Triassic (Nemcok et al., 1995) is not recorded in the soft sediment deformations, suggesting that the
535 associated faults, such as the Bristol Channel Fault (Fig. 9), were not responsible for the
536 earthquake(s) leading to the formation of the observed SSDs. Our record of the fault(s) activity as
537 shown by SSDs in the Bristol Channel Basin is nevertheless in agreement with the Triassic thickness
538 maps of the British Isles (Whittaker, 1985). In general, the Bristol Channel Basin experienced very
539 little subsidence at the end of the Triassic with renewed activity during the Early Jurassic (Whittaker,
540 1985). In contrast, the Cardigan and Caernarfon basins show thicknesses of Triassic deposits which

541 indicate strong subsidence during this time (Whittaker, 1985), which is consistent with our SSDs
542 record.

543 The N–S orientation registered in all structures in the Devon does not match with the major N–S
544 opening direction of the Wessex Basin from the Permian (Hawkes et al., 1998). The single N–S large
545 regional structure is again the Worcester Graben, but this basin lay at quite a distance toward the
546 north (Fig. 9). Indeed, the earthquakes that triggered the SSDs in Pinhay may better have occurred on
547 one of the N-S faults located immediately westward to the Pinhay Bay site, like the Pinhay Fault, the
548 Rousdon Fault, and/or the Seaton Fault. **In that case, the activity of local faults has presumably
549 overrided the basinal fault trends influence to produce apparent anomalies in the SSDs trends.**

550

551 *5.4 Implications for the tectonic activity at the Triassic–Jurassic boundary*

552 We have shown that the deformation structures have very well constrained orientations, parallel to
553 known active faults during the Late Triassic – Early Jurassic. We thus assume that the orientation
554 defined for each outcrop characterises a local "state of stress" associated with the fault activity. The
555 SSD patterns may then be used to investigate the active fault or faults system in a given area at the
556 Triassic–Jurassic boundary.

557

558 *5.4.1 Magnitude of earthquake(s)*

559 To achieve liquefaction in sediments, the magnitude of an earthquake must be greater than M_w5
560 (Ambraseys and Sarma, 1969; Wang and Manga, 2010). Numerous earthquakes of M_w5 to M_w7 have
561 already been described in tectonically active areas of extension, such as the Corinth–Patras Rift
562 (Doutsos and Poulimenos, 1992; Albin et al., 2017) and may have been characteristic of the study
563 areas in the UK during the Triassic–Jurassic transition. However, most of these earthquakes have
564 magnitudes of less than M_w5 , as is the case in the African Rift (Lindenfeld et al., 2012) and limits the
565 number of earthquakes registered by resulting SSDs. Larger earthquakes should result in a more
566 extensive imprint in the sedimentary archives than moderate ones and according to Obermeier
567 (1996), a M_w7 earthquake can liquify sediments up to 150 km distance from the epicentre. In the
568 case of high-magnitude earthquakes ($>M_w6$), the extended duration of the liquefaction phase may
569 lead to the homogenisation of the alternations, thus forming a mixed unit (Rodríguez-Pascua et al.,
570 2000). This later state is not observed in the SSDs of Triassic–Jurassic boundary in the UK, apart from
571 locally one single layer at Pinhay Bay. Thus, the magnitude of the seismic events recorded by SSDs
572 were probably most of the time not higher than M_w5 to M_w6 .

573

574 *5.4.2 A single mega-event or several moderate seismic events over a long duration?*

575 The distance between the Waterloo Bay outcrop and the Bristol Channel is over 450 km. Therefore, it
 576 is rather unlikely that a single seismic event may have produced the SSDs in the Lough Foyle, Larne,
 577 Bristol Channel and Wessex basins. Moreover, the thickness of the disturbed layers vary greatly at
 578 each locality, from 0.2 m at Lilstock, to 0.4 m at St Audrie's Bay, and 4.5 metres at Waterloo Bay,
 579 **although this has been possibly linked, at least in some localities, to local erosion (Simms, 2007, see**
 580 **above).** The thickness of the de-structured level probably depended on the lithological pattern, as
 581 stressed above, **and/or on local erosion. In addition, it may also have been (at least partly)** controlled
 582 by the duration of the liquefaction and the magnitude of the earthquake(s), which depend on the
 583 length of the fault (Madariaga and Perrier, 1991). The observed heterogeneity in (1) the thicknesses
 584 of the disturbed layers in various basins and (2) the directional associated pattern as reconstructed
 585 from SSDs support the fact that several earthquakes on local faults rather than one mega-event at the
 586 Triassic–Jurassic transition triggered the SSD patterns. Furthermore, the orientation of the structures
 587 changes in various deformed layers in a single section, as observed in the Bristol Channel Basin.
 588 **Jeram et al. (this volume) highlighted the occurrence of two deformation events in the Westbury Fm.**
 589 **and one deformation event in the Lower Cotham Member in two localities in Northern Ireland, and**
 590 **interpreted them as seismic-induced.** It is therefore most probable that the observed disturbed
 591 layers record a series of different earthquakes, associated with varied active local faults, rather than
 592 a single, mega-event. Indeed, several authors (Mayall, 1983; Hesselbo et al., 2002, 2004; Simms,
 593 2003, 2007) assigned those SSDs to earthquakes but the number of events and their origin are still
 594 debated. Mayall (1983) suggested that the SSDs observed in the UK were linked with extensive
 595 tectonic activity during Triassic and Early Jurassic. More recently, Simms (2003, 2007) suggested that
 596 the cause of the deformation was a rare M_w10 earthquake caused by a meteorite impact, **which**
 597 **remains a possible trigger for the observed SSDs.** Hesselbo et al. (2002, 2004) and Lindström et al.
 598 (2015), observed several SSDs in different localities around the Triassic–Jurassic boundary in Western
 599 Tethys that were linked to a succession of earthquakes. They related this geodynamic context with
 600 the development of the magmatic province of the North Atlantic Ocean (CAMP, Central Atlantic
 601 Magmatic Province). **Further stressing this relationship, the SSDs found in the Westbury Fm. and in**
 602 **the Lower Cotham Member in Northern Ireland and in the Bristol Channel Basin immediately**
 603 **precede an initial carbon isotope excursion correlated with the first major pulse of CAMP volcanism**
 604 **(Jeram et al., this volume).** Our detailed study of the SSDs from the UK favors the idea of a succession
 605 of earthquakes occurring during a very active tectonic period at the Triassic–Jurassic boundary, as
 606 reported by Hesselbo et al. (2002, 2004) and Lindström et al. (2015). **The lack of comparable SSDs**
 607 **anywhere in the Jurassic strata from the UK, whereas evidence of active faulting do occur (Wall and**
 608 **Jenkyns, 2004) probably relates to the intense geodynamic activity at the Triassic–Jurassic boundary.**

609

610 *5.4.3 Rifting pattern at the Triassic–Jurassic boundary during the break-up of Pangea*

611 Our SSDs study shows that there is no principal state of stress common to the entire study region in
612 the UK. On the contrary, basins of different orientations were active at the same time and were
613 bordered by faults inherited from the Caledonian and Variscan orogenies, which were successively
614 re-activated. Some local major faults, potentially active during the Jurassic, do not seem recorded by
615 the SSDs. As an example, the main normal E–W fault direction, which corresponds to the formation
616 of the Bristol Channel Basin, recorded in the Triassic deposits of the Bristol Channel area (Nemcok et
617 al., 1995) is not recorded in the studied disturbed levels. It is possible that the earthquakes
618 associated with the opening of the Bristol Channel Basin may have been too weak (e.g., lower than
619 M_w5) to be recorded, or that the fault was not very active during the deposition of the Penarth
620 Group to the base of Blue Lias. Conversely, tectonic activity in the Cardigan Bay, St George’s Channel
621 and North Celtic Sea basins, or on local faults near Pinhay Bay in Devon such as Pinhay Fault, the
622 Rousdon Fault, and/or the Seaton Fault were probably more intense at this period. The variation of
623 the directions of SSDs associated with each seismic event finally suggests that the early extension
624 phases during Pangea Break-up were characterised by the opening of multidirectional, mosaic-style
625 basins. These basins were established before better constrained and homogeneous extension
626 directions dominate. Finally, the structural framework inherited from the Caledonian and Variscan
627 orogenies certainly played an important role in the formation of these Permo-Triassic basins, at least
628 in these early extension phases.

629

630 **6. Conclusions**

631 The disturbed sedimentary layers observed at the Triassic–Jurassic boundary in the UK and Ireland
632 combine an array of criteria used to identify seismites, attesting to a seismic origin of the studied
633 SSDs. Lithology, fluid, faulting, and overpressure processes controlled the style of deformation and its
634 stratigraphic occurrence. The complete characterisation of the SSDs of the Triassic–Jurassic boundary
635 strata at the scale of several outcrops across the UK allowed us to associate the directions of SSDs to
636 the states of stress imposed by the activity of local major faults that were linked to the opening and
637 development of Triassic basins. A series of seismic events rather than a single, mega seismic shock
638 was probably responsible for the SSD formations. The variation of the directions of SSDs associated
639 with each seismic event shows that the early extension phases of the break-up of Pangea were
640 characterised by the opening of multidirectional basins, largely controlled by the inherited
641 Caledonian and Variscan tectonic pattern. We can conclude that the orientation of the SSDs in fossil

642 seismites as reconstructed by a detailed structural and field analysis is a useful and promising tool in
643 the study of past state of stress in sedimentary basins.

644

645 **Acknowledgments**

646 We warmly thank the Geological Survey of Northern Ireland for its welcome and support and
647 LONMIN (Northern Ireland) for providing full access to the Carnduff-1, Carnduff-2, NIRE 05/08-0002
648 and NIRE 05/08-0003 cores. We thank Alexis Lethiers (Sorbonne Université) for his help on the field
649 and for a part of the drawing work. Marine Laborde was funded by a Doctoral Grant from French
650 authorities hosted at Sorbonne Université and by a SEPM Student Grant. We thank Mike Simms and
651 an anonymous reviewer for their very helpful and constructive reviews.

652

653 **7. References**

- 654 Albini, P., Rovida, A., Scotti, O., Lyon-Caen, H., 2017. Large eighteenth–nineteenth century
655 earthquakes in Western Gulf of Corinth with reappraised size and location. *Bulletin of the*
656 *Seismological Society of America* 107, 1663–1687. doi:10.1785/0120160181
- 657 Allen, J.R.L., (Ed.), 1982. *Sedimentary Structures Their Character and Physical Basis Volume 2.*
658 *Developments in Sedimentology Volume 30B.* Elsevier, Amsterdam. pp. 663.
- 659 Allen, J.R.L., 1977. The possible mechanics of convolute lamination in graded sand beds. *Journal of*
660 *the Geological Society, London* 134, 19–31.
- 661 Ambraseys, N., Sarma, S., 1969. Liquefaction of soils induced by earthquakes. *Bulletin of the*
662 *Seismological Society of America* 59, 651–664.
- 663 Anderson, T.B., Parnell, J., Ruffell, A.H., 1995. Influence of basement on the geometry of Permo-
664 Triassic basins in the northwest British Isles. In: Boldy, S.A.R. (Ed.), *Permian and Triassic Rifting in*
665 *Northwest Europe.* Geological Society, London, Special Publications 91, pp. 103–122.
- 666 Audemard, F.A., De Santis, D., 1991. Survey of liquefaction structures induced by recent moderate
667 earthquakes. *Bulletin of the International Association of Engineering Geology* 44, 5–16.
- 668 Basilone, L., Sulli, A., Gasparo Morticelli, M., 2015. The relationships between soft-sediment
669 deformation structures and synsedimentary extensional tectonics in Upper Triassic deep-water

- 670 carbonate succession (Southern Tethyan rifted continental margin - Central Sicily). *Sedimentary*
671 *Geology* 344, 310–322. doi:10.1016/j.sedgeo.2016.01.010
- 672 Bazley, R.A.B., Brandon, A., Arthurs, J.W., 1997. Geology of the Country around Limavady and
673 Londonderry. Geological Survey of Northern Ireland, Technical Report. GSNI/97/1. 96 pp.
- 674 Bergerat, F., Collin, P.Y., Ganzhorn, A.-C., Baudin, F., Galbrun, B., Rouget, I., Schnyder, J. 2011.
675 Instability structures, synsedimentary faults and turbidites, witnesses of a Liassic seismotectonic
676 activity in the Dauphiné Zone (French Alps): A case example in the Lower Pliensbachian at Saint-
677 Michel-en-Beaumont. *Journal of Geodynamics* 51, 344–357.
- 678 Chadwick, R.A., 1993. Aspects of basin inversion in southern Britain. *Journal of the Geological*
679 *Society, London* 150, 311–322.
- 680 Coward, M.P., 1995. Structural and tectonic setting of the Permo-Triassic basins of northwest
681 Europe. Geological Society, London, Special Publications 91, 7–39.
682 doi:10.1144/GSL.SP.1995.091.01.02
- 683 Dechen, S., Aiping, S., 2012. Typical earthquake-induced soft-sediment deformation structures in the
684 Mesoproterozoic Wumishan Formation, Yongding River Valley, Beijing, China and interpreted
685 earthquake frequency. *Journal of Palaeogeography* 1, 71–89.
686 doi:http://dx.doi.org/10.3724/SP.J.1261.2012.00007
- 687 Deconinck, J.-F., Hesselbo, S.P., Debuisser, N., Averbuch, O., Baudin, F., Bessa, J., 2003.
688 Environmental controls on clay mineralogy of an Early Jurassic mudrock (Blue Lias Formation,
689 southern England). *International Journal of Earth Sciences* 92, 2, 255–266.
- 690 Dobson, M.R., Delanty, L., Whittington, R.J., 1982. Stratigraphy and inversion tectonics in the St.
691 Georges Channel area off SW Wales, U.K. *Geo-Marine Letters* 2, 23–30.
- 692 Doutsos, T., Poulimenos, G., 1992. Geometry and kinematics of active faults and their seismotectonic
693 significance in the western Corinth-Patras rift (Greece). *Journal of Structural Geology* 14, 689–699.
694 doi:10.1016/0191-8141(92)90126-H
- 695 Gallois, R.W., 2005. Correlation of the Triassic and Jurassic succesions proved in the Lyme Regis
696 (1901) Borehole with those exposed on the neaby Devon and Dorset coast. *Geoscience in south-west*
697 *England* 11, 99–105.
- 698 Gallois, R.W., 2007. Stratigraphy of the of the Penarth Group (Late Triassic) revision of the the East
699 Devon coast. *Geoscience in south-west England* 11, 287–297.

- 700 Gallois, R.W., 2009. Lithostratigraphy of the Penarth Group (Late Triassic) of the Severn Estuary area.
701 *Geoscience in south-west England* 12, 71–84.
- 702 Ghosh, S.K., Pandey, A.K., Pandey, P., Ray, Y., Sinha, S., 2012. Soft-sediment deformation structures
703 from the Paleoproterozoic Damtha Group of Garhwal Lesser Himalaya, India. *Sedimentary Geology*
704 261–262, 76–89. doi:10.1016/j.sedgeo.2012.03.006
- 705 Greb, S.F., Archer, A.W., 2007. Soft-sediment deformation produced by tides in a meizoseismic area,
706 Turnagain Arm, Alaska. *Geology* 35, 435–438. doi:10.1130/G23209A.1
- 707 Hallam, A., 1960. The White Lias of the Devon coast. *Proceedings of the Geologists' Association* 71,
708 47–60. doi:10.1016/S0016-7878(60)80031-4
- 709 Hawkes, P.W., Fraser, A.J., Einchcomb, C.C.G., 1998. The tectono-stratigraphic development and
710 exploration history of the Weald and Wessex basins, Southern England, UK. Geological Society,
711 London, Special Publications 133, 39–65. doi:10.1144/GSL.SP.1998.133.01.03
- 712 Hesselbo, S.P., Robinson, S.A., Surlyk, F., Piasecki, S., 2002. Terrestrial and marine extinction at the
713 Triassic-Jurassic boundary synchronized with major carbon-cycle perturbation: A link to initiation of
714 massive volcanism? *Geology* 30, 251. doi:10.1130/0091-7613(2002)030<0251:TAMEAT>2.0.CO;2
- 715 Hesselbo, S.P., Robinson, S.A., Surlyk, F., 2004. Sea-level change and facies development across
716 potential Triassic – Jurassic boundary horizons , SW Britain. *Journal of the Geological Society, London*
717 161, 365–379.
- 718 Holdsworth, R.E., Woodcock, N.H., Strachan, R.A., 2012. Geological Framework of Britain and Ireland.
719 In: Woodcock, N., Strachan, R. (Eds.), *Geological History of Britain and Ireland, Second Edition*. pp.
720 19–39, Blackwell Publishing Ltd., Oxford.
- 721 Homberg, C., Schnyder, J., Benzaggagh, M. Late Jurassic-Early Cretaceous faulting in the Southeastern
722 French Basin: does it reflect a tectonic reorganization? (2013). *Bulletin de la Société Géologique de*
723 *France*, 184, 4-5, p.501-514.
- 724 Ivimey-Cook, H.C., 1974. The Permian and Triassic deposits of Wales. In: Owen, T.R. (Ed.), *The Upper*
725 *Paleozoic and Post Paleozoic Rocks of Wales*. pp. 295–321. University of Wales Press, Cardiff.
- 726 Jeram, A., Simms, M.J., Hesselbo, S.P., Raine, R., 2020. Carbon isotopes, ammonites and earthquakes:
727 Key Triassic-Jurassic boundary events recorded in coastal sections of South East County Antrim,
728 Northern Ireland, UK. *Proceedings of the Geologists' Association*. This volume.

- 729 Ken-Tor, R., Agnon, A., Enzel, Y., Stein, M., Marco, S., Negendank, J.F.W., 2001. High-resolution
730 geological record of historic earthquakes in the Dead Sea basin. *Journal of Geophysical Research* 106,
731 2221–2234.
- 732 Kullberg, J.C., Olóriz, F., Marques, B., Caetano, P.S., Rocha, R.B., 2001. Flat-pebble conglomerates: A
733 local marker for early jurassic seismicity related to syn-rift tectonics in the Sesimbra area (Lusitanian
734 Basin, Portugal). *Sedimentary Geology* 139, 49–70. doi:10.1016/S0037-0738(00)00160-3
- 735 Le Roux, J.P., Nielsen, S.N., Kemnitz, H., Henriquez, Á., 2008. A Pliocene mega-tsunami deposit and
736 associated features in the Ranquil Formation, southern Chile. *Sedimentary Geology* 203, 164–180.
737 doi:10.1016/j.sedgeo.2007.12.002
- 738 Lindenfeld, M., Rumpker, G., Batte, A., Schumann, A., 2012. Seismicity from February 2006 to
739 September 2007 at the Rwenzori Mountains, East African Rift: Earthquake distribution, magnitudes
740 and source mechanisms. *Solid Earth* 3, 251–264. doi:10.5194/se-3-251-2012
- 741 Lindström, S., Pedersen, G.K., Van De Schootbrugge, B., Hansen, K.H., Kuhlmann, N., Thein, J.,
742 Johansson, L., Petersen, H.I., Alwmark, C., Dybkjær, K., Weibel, R., Erlström, M., Nielsen, L.H.,
743 Oschmann, W., Tegner, C., 2015. Intense and widespread seismicity during the end-Triassic mass
744 extinction due to emplacement of a large igneous province. *Geology* 43, 387–390.
745 doi:10.1130/G36444.1
- 746 Lowe, D.R., 1976. Subaqueous liquefied and fluidized sediment flows and their deposits.
747 *Sedimentology* 23, 285–308. doi:10.1111/j.1365-3091.1976.tb00051.x
- 748 Lowe, D.R., 1975. Water escape structures in coarse-grained sediments. *Sedimentology* 22, 157–204.
749 doi:10.1111/j.1365-3091.1975.tb00290.x
- 750 Madariaga, R., Perrier, G., 1991. *Les tremblements de terres*, Presses du CNRS, Paris. pp. 210.
- 751 Marco, S., Stein, M., Agnon, A., 1996. Long-term earthquake clustering: A 50,000-year paleoseismic
752 record in the Dead Sea Graben. *Journal of Geophysical Research* 101, 6179–6191.
753 doi:10.1029/95JB01587
- 754 Mayall, M.J., 1983. An earthquake origin for synsedimentary deformation in a late Triassic (Rhaetian)
755 lagoonal sequence, southwest Britain *Sedimentary Deformation Desiccation Cracks*. *Geological*
756 *Magazine* 120, 613–622.
- 757 Mitchell, W.I. (Ed.), *The Geology of Northern Ireland –Our Natural Foundation (Second Edition)*,
758 2004. Geological Survey of Northern Ireland Belfast.

- 759 Molina, J.M., Alfaro, P., Moretti, M., Soria, J.M., 1998. Soft-sediment deformation structures induced
760 by cyclic stress of storm waves in tempestites (Miocene, Guadalquivir Basin, Spain). *Terra Nova*, 10,
761 145–150.
- 762 Montenat, C., Barrier, P., Ott d'Estevou, P., Hibsich, C., 2007. Seismites: An attempt at critical analysis
763 and classification. *Sedimentary Geology* 196, 1–4, 5–30.
- 764 Nanayama, F., Shigeno, K., Satake, K., Shimokawa, K., Koitabashi, S., Miyasaka, S., Ishii, M., 2000.
765 Sedimentary differences between the 1993 Hokkaido-nansei-oki tsunami and the 1959 Miyakojima
766 typhoon at Taisei, southwestern Hokkaido, northern Japan. *Sedimentary Geology* 135, 255–264.
767 doi:10.1016/S0037-0738(00)00076-2
- 768 Nemcok, M., Gayer, R., Miliorizos, M., 1995. Structural analysis of the inverted Bristol Channel Basin:
769 implications for the geometry and timing of fracture porosity. Geological Society, London, Special
770 Publications 88, 355–392. doi:10.1144/GSL.SP.1995.088.01.20
- 771 Obermeier, S.F., 1996. Use of liquefaction-induced features for paleoseismic analysis — An overview
772 of how seismic liquefaction features can be distinguished from other features and how their regional
773 distribution and properties of source sediment can be used to infer the location and strength of
774 Holocene paleo-earthquakes. *Engineering Geology* 44, 1–76. doi:10.1016/S0013-7952(96)00040-3
- 775 Owen, G., 1987. Deformation processes in unconsolidated sands. In: Jones, M.E., Prestpn, R.M.F.
776 (Eds.), *Deformation of Sediments and Sedimentary Rocks*. Geological Society, London, Special
777 Publications 29, pp. 11–24.
- 778 Owen, G., Moretti, M., 2011. Identifying triggers for liquefaction-induced soft-sediment deformation
779 in sands. *Sedimentary Geology* 235, 141–147. doi:10.1016/j.sedgeo.2010.10.003
- 780 Plaziat, J.C., Ahmamou, M., 1998. Les différents mécanismes à l'origine de la diversité des séismites ,
781 leur identification dans le Pliocène du Saïs de Fès et de Meknès (Maroc) et leur signification
782 tectonique. *Geodinamica Acta* 11, 183–203. doi:10.1016/S0985-3111(98)80004-1
- 783 Pope, M.C., Read, J.F., Hofmann, H.J., Bambach, R., 1997. Late Middle to Late Ordovician seismites of
784 Kentucky, southwest Ohio and Virginia: Sedimentary recorders of earthquakes in the Appalachian
785 basin. *GSA Bulletin* 109, 489–503. doi:10.1130/0016-7606(1997)109<0489
- 786 Radley, J.D., Carpenter, S.C., 1998. The late triassic strata of Manor Farm, Aust, South
787 Gloucestershire, in: *Proceedings of the Bristol Naturalists' Society* 58, pp. 57–68.

- 788 Radley, J.D., Swift, A., 2002. "Sedimentology of the Triassic-Jurassic boundary beds in Pinhay
789 Bay(Devon, SW England)" by P. B. Wignall: comment. *Proceedings of the Geological Association* 113,
790 271–272. doi:10.1016/S0016-7878(02)80029-3
- 791 Raine, R.J., Copestake, P., Simms, M.J., Boomer, I., 2020. Uppermost Triassic to Lower Jurassic
792 sediments of the island of Ireland and its surrounding basins. *Proceedings of the Geologists'
793 Association*. This volume.
- 794 Richardson, L., 1911. The Rhaetic and contiguous deposits of West, Mid and part of East Somerset.
795 *Quarterly Journal of the Geological Society* 67, 1–74.
- 796 Rodríguez-Pascua, M.A., Calvo, J.P., De Vicente, G., Gómez-Gras, D., 2000. Soft-sediment deformation
797 structures interpreted as seismites in lacustrine sediments of the Prebetic Zone, SE Spain, and their
798 potential use as indicators of earthquake magnitudes during the Late Miocene. *Sedimentary Geology*
799 135, 117–135. doi:10.1016/S0037-0738(00)00067-1
- 800 Ruffell, A., Shelton, R., 1999. The control of sedimentary facies by climate during phases of crustal
801 extension: Examples from the Triassic of onshore and offshore England and Northern Ireland. *Journal
802 of the Geological Society, London* 156, 779–789. doi:10.1144/gsjgs.156.4.0779
- 803 Schnyder, J., Baudin, F., Deconinck, J.F., 2005. A possible tsunami deposit around the Jurassic-
804 Cretaceous boundary in the Boulonnais area (northern France). *Sedimentary Geology* 177, 209–227.
805 doi:10.1016/j.sedgeo.2005.02.008
- 806 Simms, M.J., 2003. Uniquely extensive seismite from the latest Triassic of the United Kingdom :
807 Evidence for bolide impact ? *Geology* 31, 557–560. doi:10.1130/0091-7613(2003)031<0557
- 808 Simms, M.J., 2007. Uniquely extensive soft-sediment deformation in the Rhaetian of the UK:
809 Evidence for earthquake or impact? *Palaeogeography Palaeoclimatology Palaeoecology* 244, 407–
810 423. doi:10.1016/j.palaeo.2006.06.037
- 811 Simms, M.J., Jeram, A.J., 2007. Waterloo Bay, Larne, Northern Ireland: a candidate Global Stratotype
812 Section and Point for the base of the Hettangian Stage and Jurassic System. *ISJS Newsletter* 34, 50–
813 68. Stoneley, R., 1982. The structural development of the Wessex Basin. *Journal of the Geological
814 Society, London* 139, 543–554. doi:10.1144/gsjgs.139.4.0543
- 815 **Storrs, G., W., 1994. Fossil vertebrate faunas of the British Rhaetian (latest Triassic). *Zoological
816 Journal of the Linnean Society*, 112, Issue 1-2, 217–259.**

- 817 Swift, A., 1995. A review of the nature and outcrop of the “White Lias” facies of the Langport
818 Member (Penarth Group: Upper Triassic) in Britain. *Proceedings of the Geologists' Association* 106,
819 247–258. doi:10.1016/S0016-7878(08)80236-2
- 820 Swift, A., Martill, D.M., (Eds.), 1999. *Fossils of the Rhetian Penarth Group*. Palaeontological
821 Association, London.
- 822 Takashimizu, Y., Masuda, F., 2000. Depositional facies and sedimentary successions of earthquake-
823 induced tsunami deposits in Upper Pleistocene incised valley fills, central Japan. *Sedimentary*
824 *Geology* 135, 231–239. doi:10.1016/S0037-0738(00)00074-9
- 825 Tappin, D.R., Chadwick, R.A., Jackson, A.A., Wingfield, R.T.R., Smith, N.J.P, 1994. *The geology of*
826 *Cardigan Bay and the Bristol Channel*. HMSO, London, pp. 107.
- 827 Tessier, B. and Terwindt, J., 1994. An Example of Soft-Sediment Deformations in an Intertidal
828 Environment - The Effect of a Tidal Bore. *Comptes-Rendus de l'Académie des Sciences Série II*, 217-
829 233.
- 830 **Wall, G.R.T. and Jenkyns, H.C., 2004. The age, origin and tectonic significance of Mesozoic sediment-**
831 **filled fissures in the Mendip Hills (SW England): implications for extension models and Jurassic sea-**
832 **level curve. *Geological Magazine*, 141, 471-504.**
- 833 Wang, C.-Y., Manga, M., 2010. Hydrologic responses to earthquakes and a general metric. *Geofluids*
834 206–216. doi:10.1111/j.1468-8123.2009.00270.x
- 835 Warrington, G., Audley, M.G., Elliot, R.E., 1980. *A correlation of Triassic Rocks in the British Isles*.
836 Geological Society, London, Special Report 13.
- 837 Warrington, G., Cope, J.C.W., Ivimey-Cook, H.C., 1994. St Audrie's Bay, Somerset, England: a
838 candidate Global Stratotype Section and Point for the base of the Jurassic System. *Geological*
839 *Magazine* 131, 191–200. doi:10.1017/S0016756800010724
- 840 Waters, R.A., Lawrence, D.J.D. 1987. *Geology of the South Wales Coalfield, Part III, the country*
841 *around Cardiff*. Memoir for 1:50 000 geological sheet 263 (England and Wales). Third Edition. HMSO,
842 London. pp. 114.
- 843 Wheeler, R.L., 2002. Distinguishing seismic from nonseismic soft-sediment structures: Criteria from
844 seismic-hazard analysis. In: Etensohn, F.R., Rast, N., Brett, C.E. (Eds.), *Ancient Seismites*. Geological
845 Society of America, Special Papers 359. GSA, Boulder, Colorado, pp. 1–11.

846 Whittaker, A., 1985. Isopachytes for the Mercia Mudstone Group plus Penarth Group. In: Whittaker,
847 A. (Ed.), Atlas of Onshore Sedimentary Basins in England and Wales. Blackie & Son Limited, Glasgow,
848 pp. 80.

849 Wignall, P.B. 2001 Sedimentology of the Triassic-Jurassic boundary beds in Pinhay Bay (Devon, SW
850 England). Proceedings of the Geologists' Association 112, 349–360.

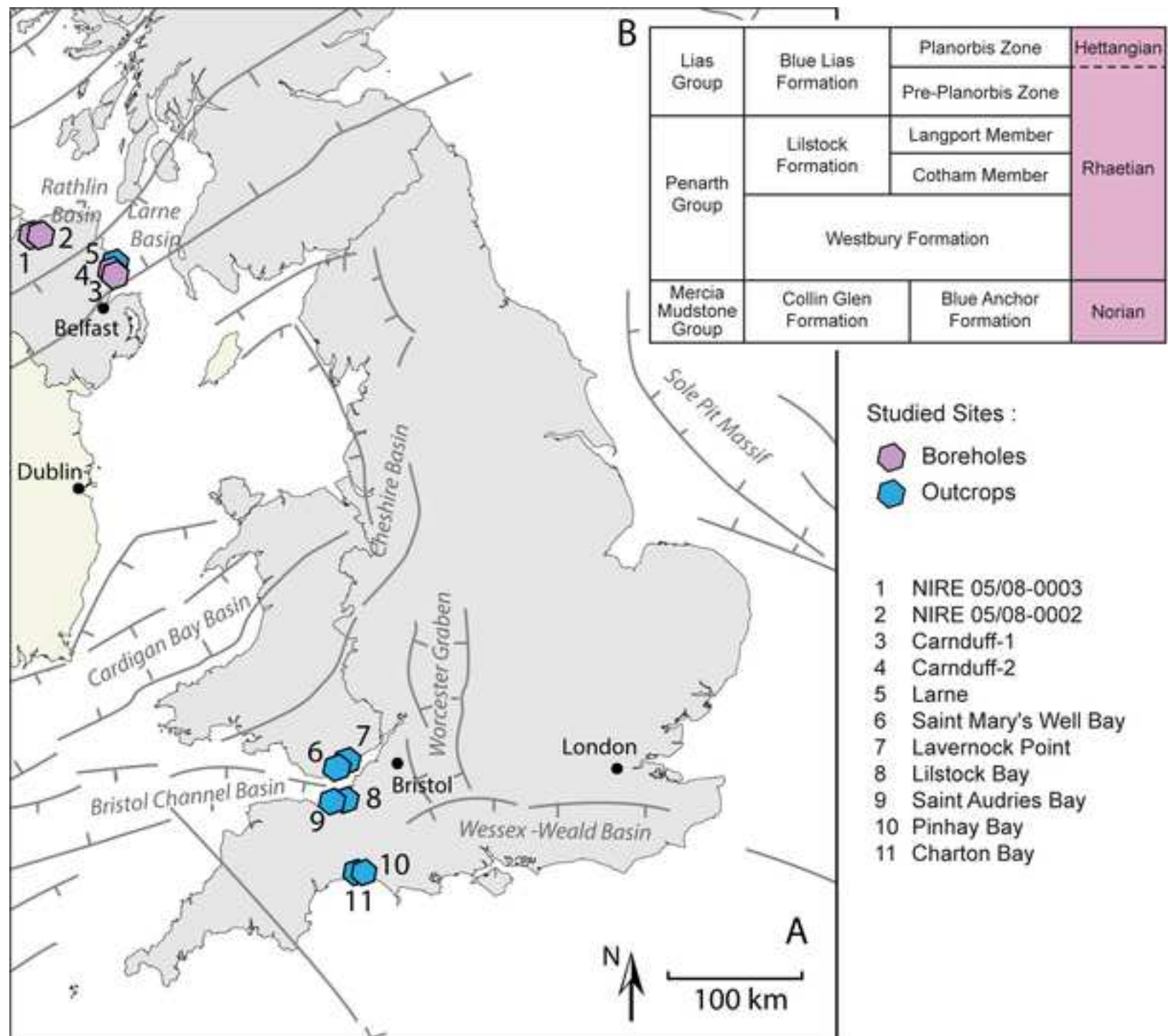
851 Ziegler, P.A., Stampfli, G.M., 2001. Late Paleozoic-Early Mesozoic plate boundary reorganisation:
852 collapse of the variscan orogen and opening of Neothetys., in: Cassinis, G. (Ed.), Permian Continental
853 Deposits of Europe and Other areas. Regional Reports and Correlations. pp. 17–34.

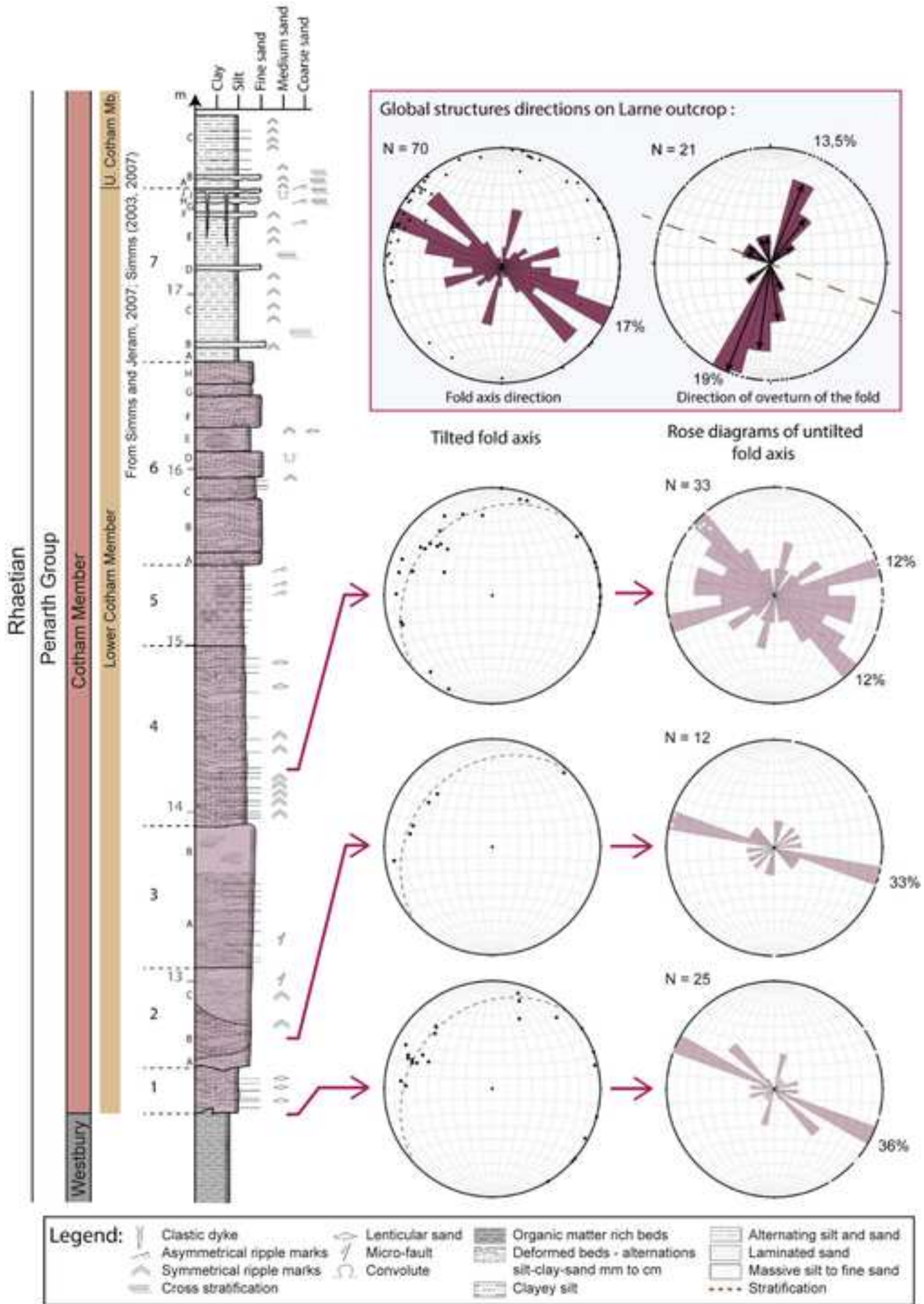
854 Ziegler, P. a., Dezes, P., 2006. Crustal evolution of Western and Central Europe. Geological Society,
855 London, Memoirs 32, 43–56. doi:10.1144/GSL.MEM.2006.032.01.03

856

857

858





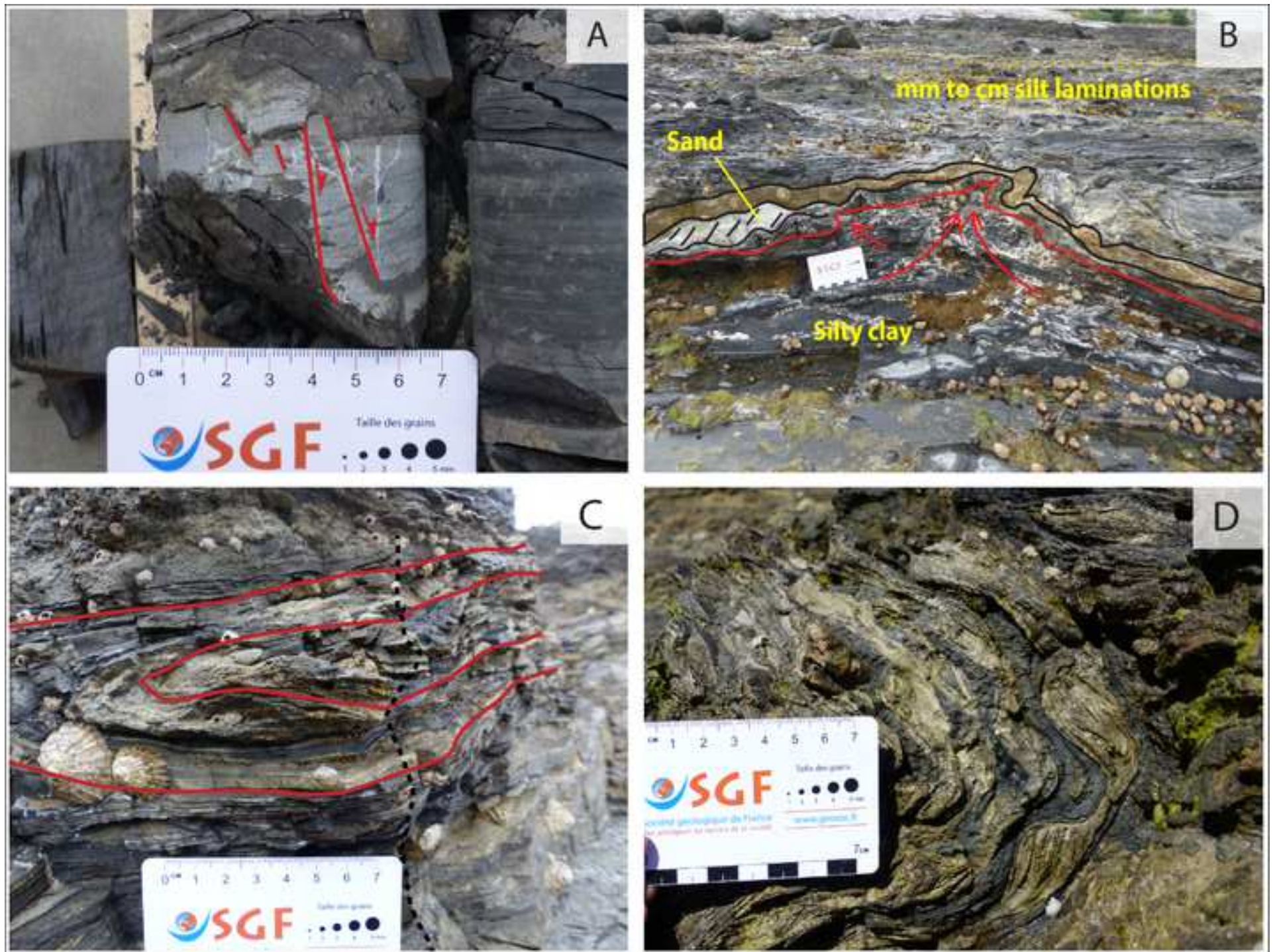
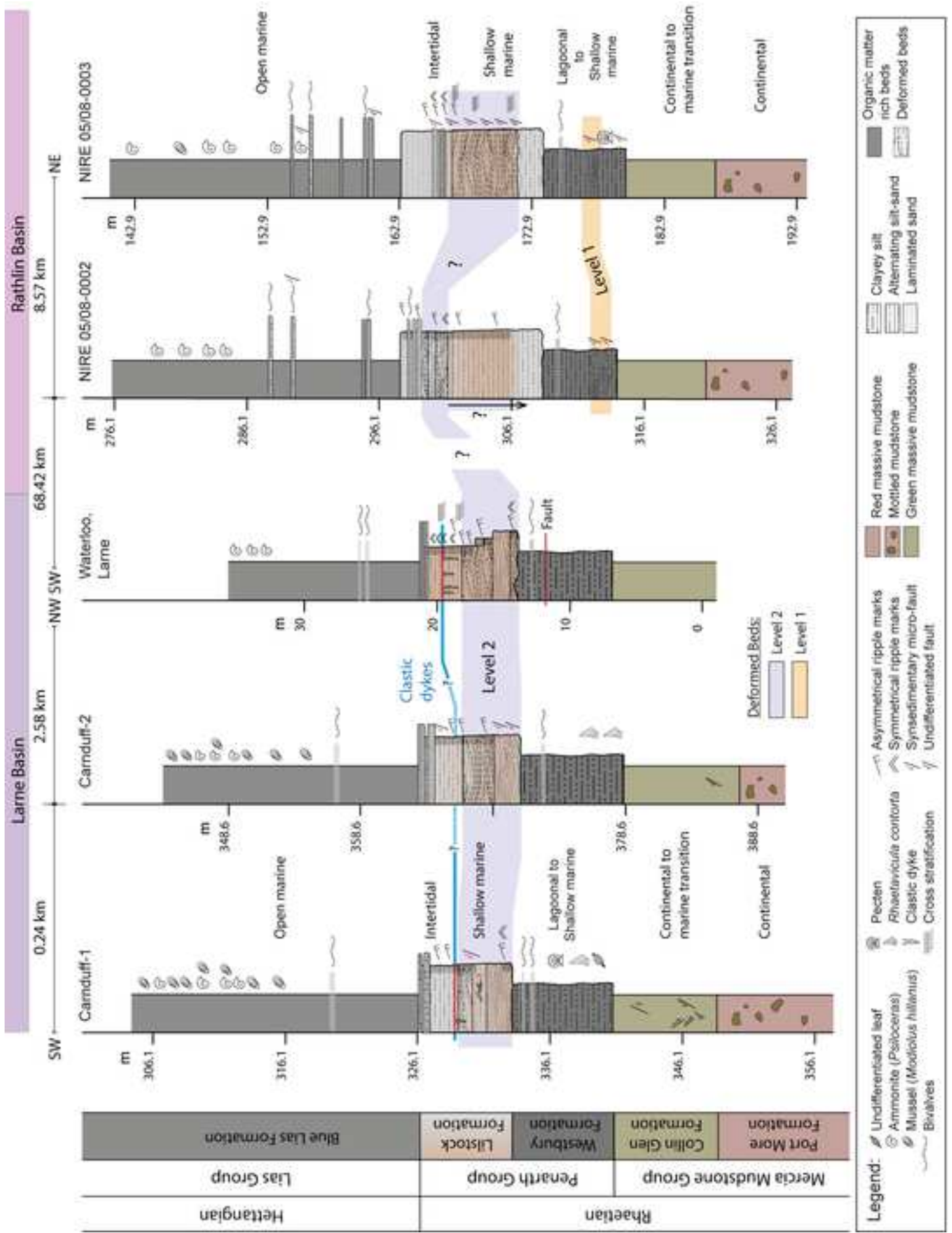
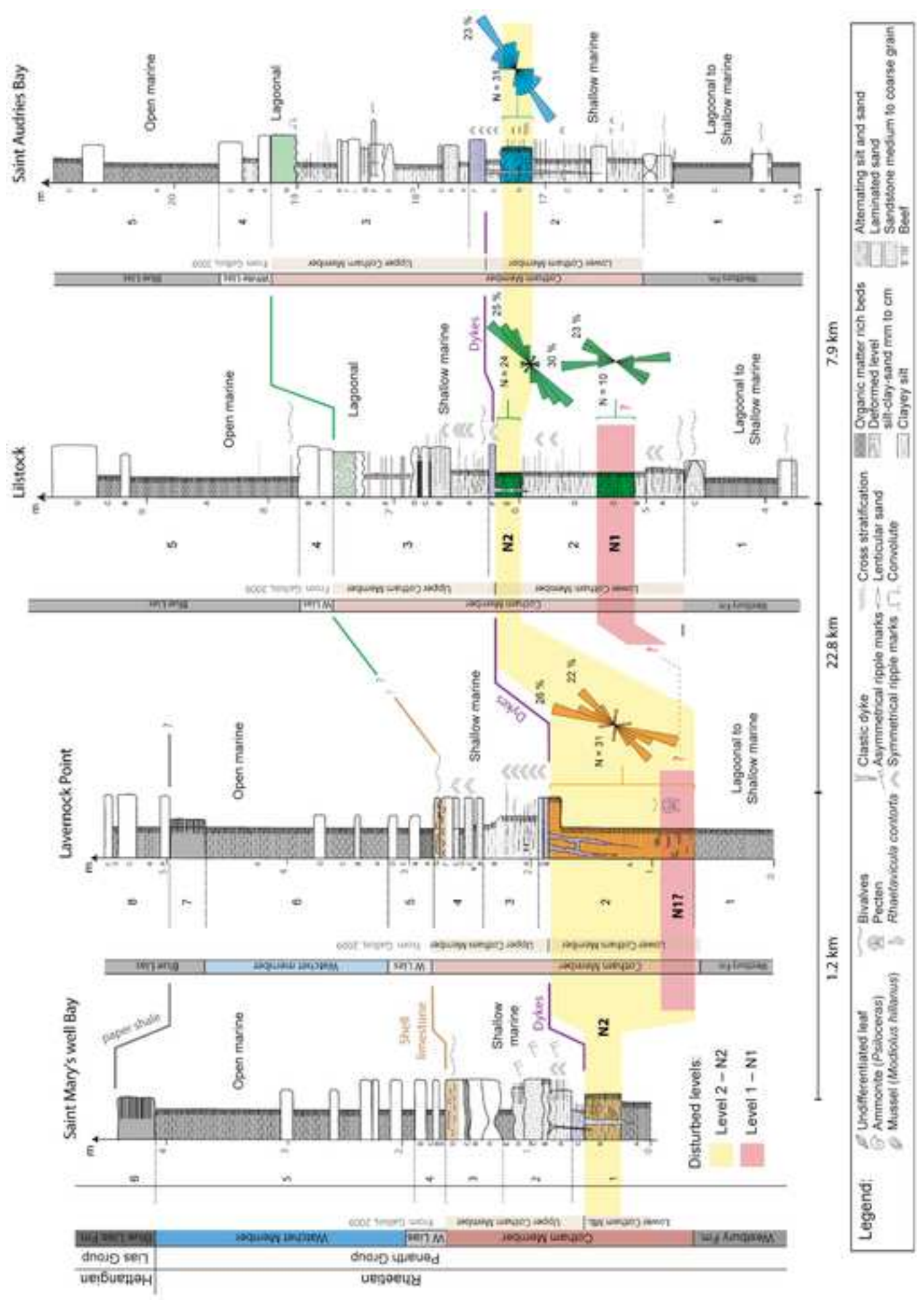
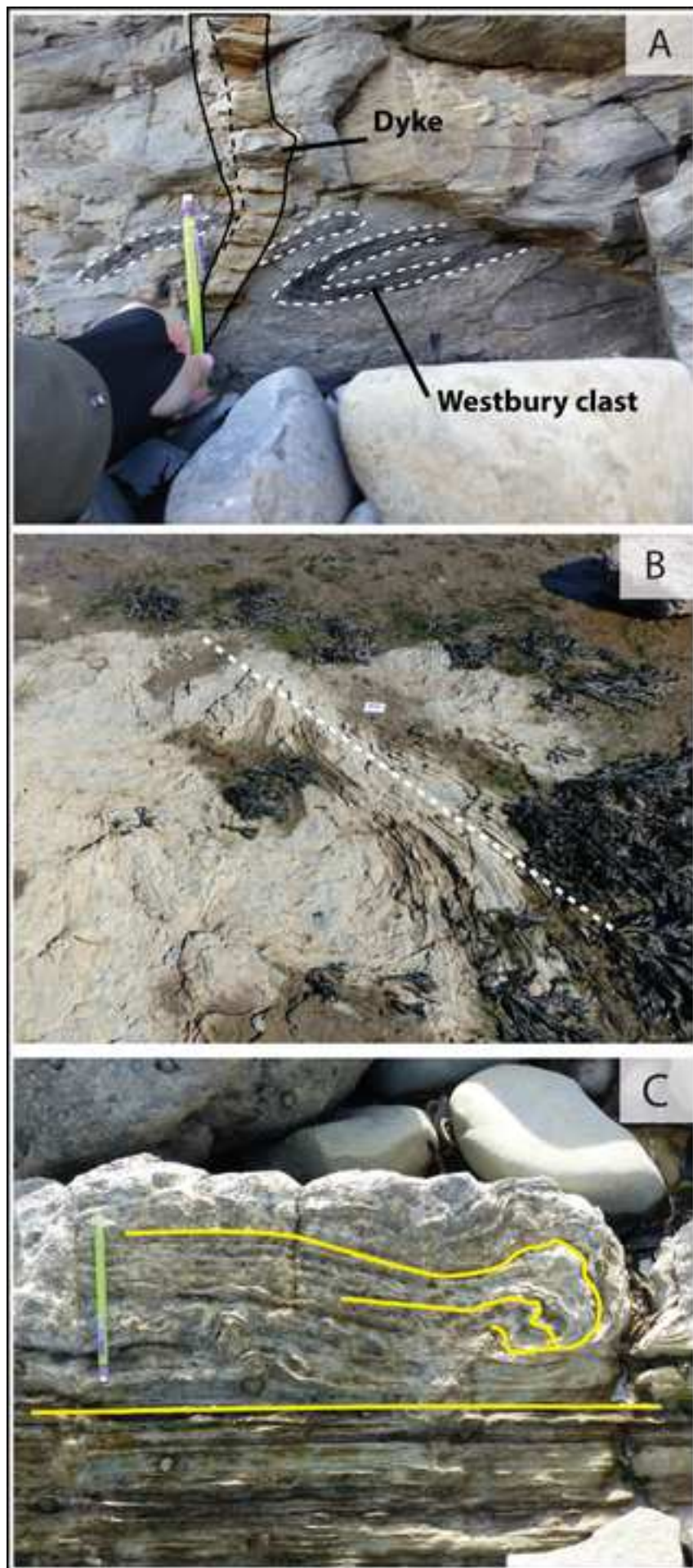


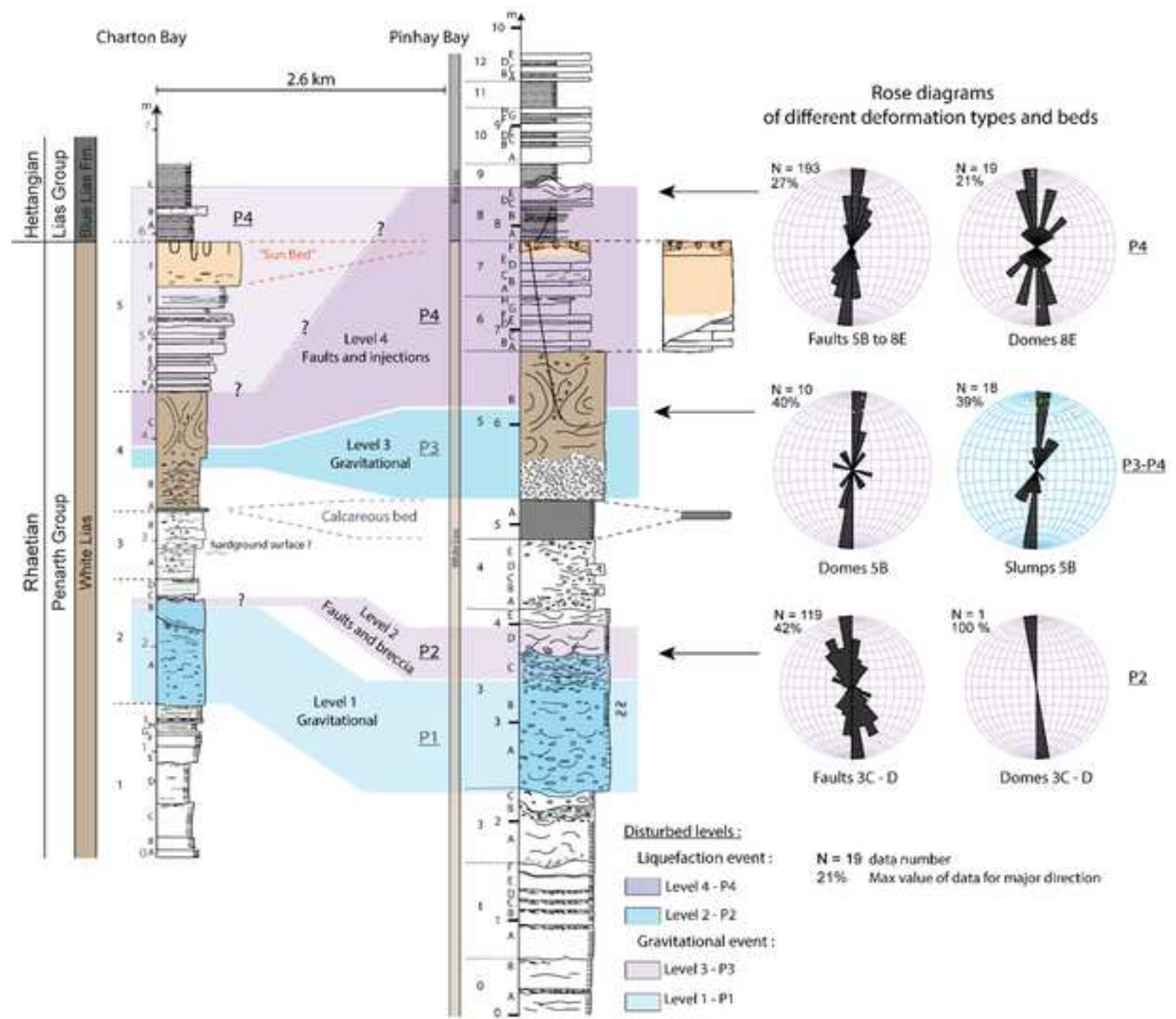
Figure 4

[Click here to access/download;Figure;Fig 4.tif](#)









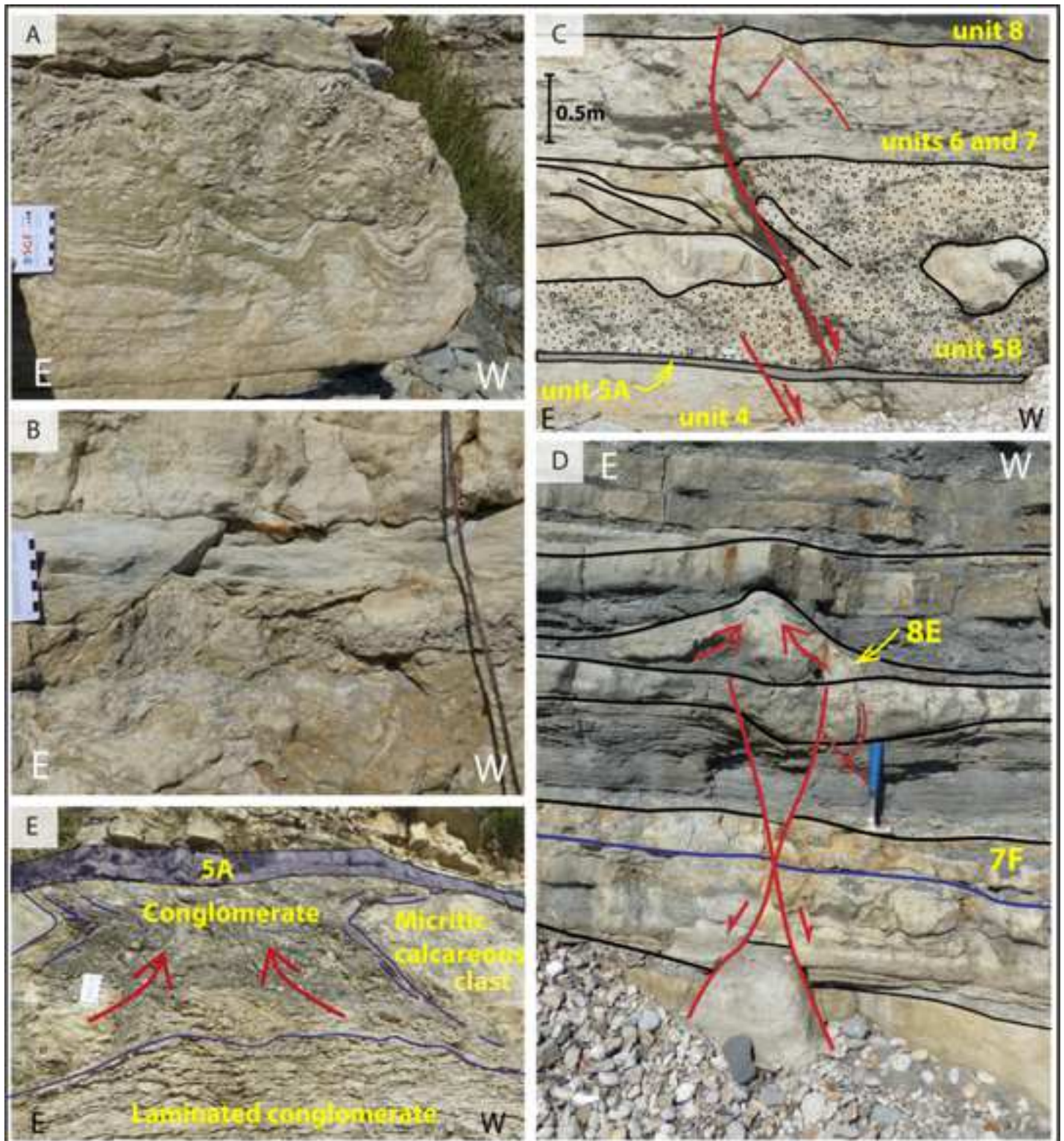
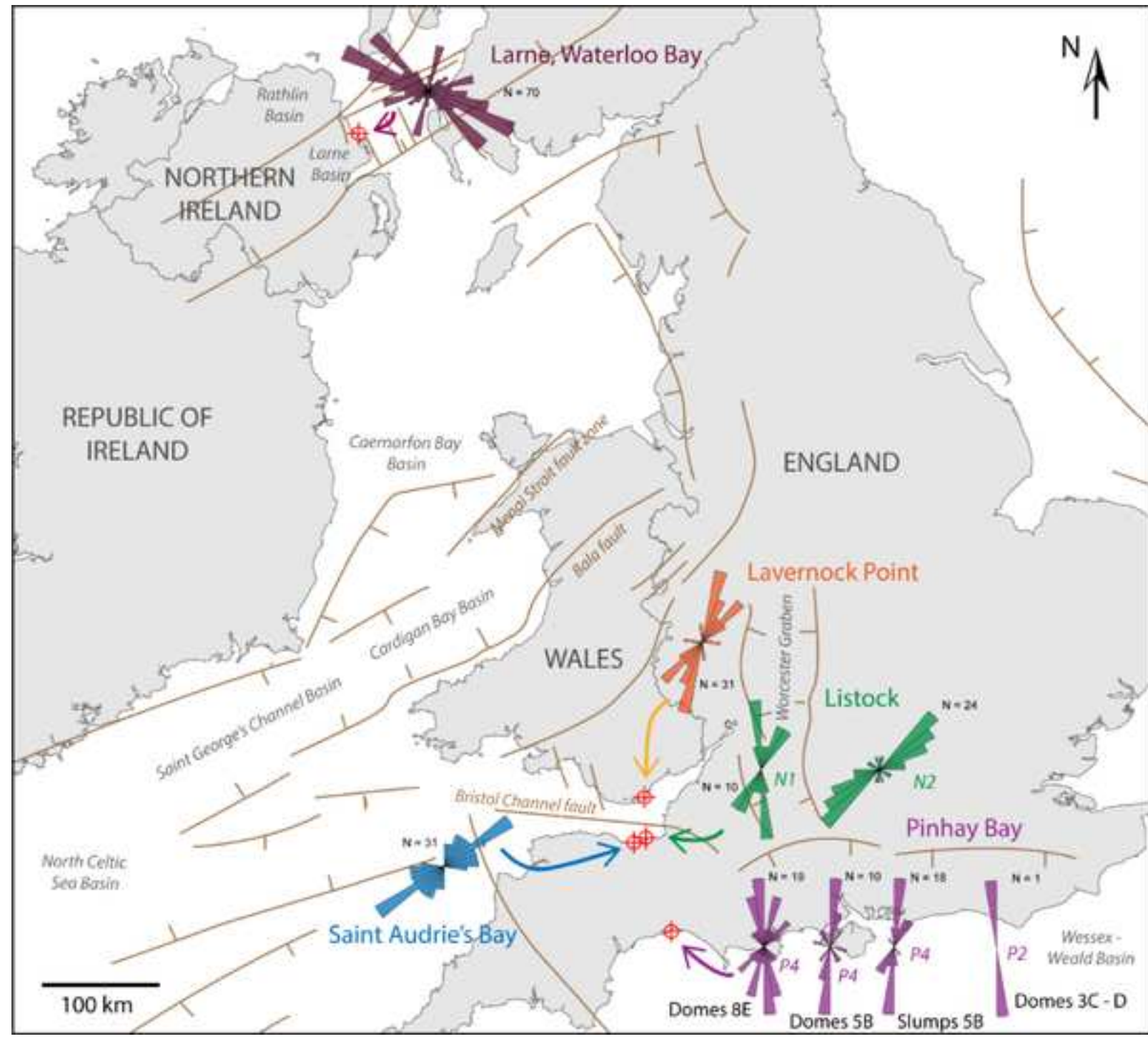


Figure 9



Declaration of interests

The authors declare that they have no known competing financial interests or personal relationships that could have appeared to influence the work reported in this paper.

The authors declare the following financial interests/personal relationships which may be considered as potential competing interests: